



DET NORSKE VERITAS

Final Report

Dissecting Coating Disbondments

Pipeline and Hazardous Materials Safety Administration
U.S. Department of Transportation

Report No./DNV Reg No.: ENAUS 811 Brossia (101131)
Rev 1


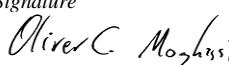



Dissecting Coating Disbondments	<p>DNV COLUMBUS, INC. Materials & Corrosion Technology Center 5777 Frantz Road Dublin, OH 43017-1386, United States Tel: (614) 761-1214 Fax: (614) 761-1633 http://www.dnv.com http://www.dnvcolumbus.com</p>
For: Pipeline and Hazardous Materials Safety Administration – Office of Pipeline Safety U.S. Department of Transportation	
Account Ref.:	

Date of First Issue:	March 2009	Project No.	
Report No.:		Organization Unit:	Materials & Corrosion Technology Center
Revision No.:	1	Subject Group:	

Summary:

A study was conducted to evaluate the main factors that lead to pipeline coating disbondment. This study compared laboratory and field observations to help ensure the validity of the findings.

Prepared by:	<i>Name and Position</i> Sean Brossia Principle Engineer	<i>Signature</i> 
Verified by	<i>Name and Position</i> Oliver Moghissi Director - MCTC	<i>Signature</i> 
Approved by:	<i>Name and Position</i> Oliver Moghissi Director - MCTC	<i>Signature</i> 

<input type="checkbox"/>	No distribution without permission from the client or responsible organizational unit (however, free distribution for internal use within DNV after 3 years)	Indexing Terms	
<input type="checkbox"/>	No distribution without permission from the client or responsible organizational unit	Key Words	
<input type="checkbox"/>	Strictly confidential	Service Area	
X	Unrestricted distribution	Market Segment	

Rev. No. / Date:	Reason for Issue:	Prepared by:	Approved by:	Verified by
1 November 31 2010	Final formatting	Sean Brossia	Oliver Moghissi	Oliver Moghissi

© 2010 DNV Columbus, Inc.

All rights reserved. This publication or parts thereof may not be reproduced or transmitted in any form or by any means, including photocopying or recording, without the prior written consent of DNV Columbus, Inc.

Table of Contents

EXECUTIVE SUMMARY	1
1 LIST OF ABBREVIATIONS.....	2
2 INTRODUCTION AND BACKGROUND.....	3
2.1 Introduction.....	3
2.2 Background.....	3
3 DEVELOPMENT OF A TEST METHODOLOGY TO CHARACTERIZE COATING DISBONDMENTS	5
3.1 Analysis of the critical variables.....	5
3.1.1 Adhesion strength.....	5
3.1.2 Surface pH.....	7
3.1.3 Coating underside chemistry	7
3.1.4 Anchor pattern	7
3.1.5 Demonstration of the procedure in actual pipe sections.....	8
4 CHARACTERIZATION OF AVAILABLE AND ADDITIONAL PIPE SECTIONS.....	12
4.1 Cathodic Disbondment Tests (CDT) on New and Aged Pipe Sections.....	17
4.1.1 CDT on new pipe section and coupons	18
4.1.1.1 New Pipe Sections	18
4.1.2 CDT on aged pipe sections.....	29
4.1.3 CDT on flat coupons	35
5 ON-SITE ANALYSIS	44
6 DISCUSSION	49
7 CONCLUSIONS.....	51
8 REFERENCES	51

EXECUTIVE SUMMARY

Coatings are the primary means for imparting corrosion protection to gas and liquid pipelines. Though cathodic protection is also often applied, if no coating was present the demand for supplied current to effectively cathodically protect the pipe would be cost-prohibitive. Because coatings are the main line of defense, understanding how they disbond from the pipe and lead to defects and flaws which in turn could result in subsequent corrosion is important.

In this project laboratory-generated results were compared to coating failures observed on pipe segments that had been taken out of service as well as in-ditch evaluations. By examining variables such as coating chemistry, surface chemistry and contamination, surface roughness, and anchor pattern a standardized experimental procedure aimed to evaluate the main causes leading to coating disbondment was developed and validated. Using this approach, the following conclusions were made:

1. Areas affected by cathodic disbondment on fusion bonded epoxy and coal tar enamel coatings tended to also exhibit low adhesion strength.
2. Highly alkaline conditions, as has been proposed to aid in the disbondment process, were observed during cathodic disbondment tests but only in the region immediately adjacent to the defect. At even small distances away from the defect, the pH was nearly neutral.
3. During cathodic disbondment testing, the disbondment often times extended beyond the initial exposed area of the test.

1 LIST OF ABBREVIATIONS

Term	Abbreviation
Cathodic Disbondment test	CDT
Cathodic Protection	CP
Coat Tar Enamel	CTE (CT)
Electrochemical Impedance Spectroscopy	EIS
Fusion Bond Epoxy	FBE
Ion Exchange Chromatography	IEC
Low Frequency Impedance	LFI
Reinforced Coal Tar Enamel	RCTE

2 INTRODUCTION AND BACKGROUND

2.1 Introduction

Coatings are the primary means for imparting corrosion protection to gas and liquid pipelines. Though cathodic protection is also often applied, if no coating was present the demand for supplied current to effectively cathodically protect the pipe would be cost-prohibitive. Because coatings are the main line of defense, understanding how they disbond from the pipe and lead to defects and flaws which in turn could result in subsequent corrosion is important.

The objective of this project was to identify the conditions promoting coating disbondment during in-service exposure. A set of variables including coating chemistry, surface chemistry, surface roughness, anchor pattern, coating underside chemistry, and optical analysis was investigated and the critical parameters leading to disbondment evaluated. Developing a better understanding of the coating disbondment process, especially concerning the initial stages of coating degradation, gained during the project will serve as a stepping stone for developing a field-based methodology to predict long-term coating performance and to identify the onset of disbondment.

2.2 Background

Buried pipelines are protected from the aggressive environment by non-metallic coatings and, in most cases, by cathodic protection (CP). Adhesion of the coating to the substrate has been identified as the most important variable for service [1-8]. Thus, maintaining adhesion over long periods of time under adverse conditions represents a major engineering challenge with immediate relevance.

Chemical adhesion of a coating to any given substrate depends on the number of active bonding sites [9]. In most environments steel surfaces will usually contain metal ions, oxides, and hydroxides. Pairing of hydroxides with OH⁻ groups generate an additional attractive force (known as hydrogen bonding). Hydrogen bonds are typically 3 times stronger than weaker Van der Waals bonds. This additional attractive force gives fusion bond epoxy (FBE) coatings their superior strength when compared against coal tar or asphalt based coatings [9].

Several factors such as ground water chemistry, CP level, CP by-products, soil chemistry, and surface roughness (anchor pattern), surface contamination, pipe bending, and the presence of defects can significantly affect adhesion [10-11]. From all these variables, previous work suggested that both the anchor pattern and the presence of surface contamination were the most significant [10]. In general, clean and sand blasted pipe surfaces tend to show the highest adhesive strength. Likewise, from the different types of surface contaminants, chloride salts have

been shown to have the most detrimental effects on adhesion during ASTM standard cathodic disbondment tests.

Corrosion under coating disbondments is an insidious phenomenon because it is difficult to detect using conventional above ground techniques [11]. Coating disbondment occurs when all adhesive forces have been lost locally [6]. Although a definitive explanation for the initiation coating disbondment has yet to be proposed, there seems to be an agreement on that adhesion between the coating and the steel surface is affected by the high pH evolving as a consequence of CP on areas where bare steel is exposed.

Several models have been proposed to describe the migration of ionic species inside disbonded regions and the environment resulting from such transport phenomenon [6, 11-15]. In a recent publication, using computer simulations Song and Sridhar [12] showed that, in the presence of CP, the pH inside the crevice increases with time. If sufficient time is allowed, the pH deeper in the crevice became higher than near the holiday. Likewise, an $O_2(g)$ concentration cell can form in the crevice, which in turn determines corrosion rates. According to the authors, the ionic current generated by the differential $O_2(g)$ content along the crevice results in a deeper penetration and, therefore, in a more severe corrosion activity. If the crevice is saturated by ferrous hydroxide, the effects of $CO_2(g)$ were shown to be minimal. At high partial pressures, however, the effects of $CO_2(g)$ are suggested to be significant. Song and Sridhar also studied the effects of solution flow along disbondments [12] to model the flow patterns observed in the field and reported in [16]. For this model the authors simulated two holidays connected through a one-dimensional disbonded path. Computational simulation showed that a peak corrosion rate occurred at the in-flow holiday for any given flow rate, which increased with increased flow velocity. Perdomo and Song [6] studied the environment under disbonded coatings using simulated crevice geometries. The authors placed microelectrodes along the artificial crevice and measured the time evolution of potential and pH. In accordance with the work of Song and Sridhar, the authors found that a differential aeration cell develops, consuming $O_2(g)$ and increasing pH deep in the crevice. The authors also pointed out the influence of high IR drop, which could lead to CP shielding under certain conditions.

Although the effort conducted to date have lead to a better understanding of the environment developing under disbondments, all the models and laboratory investigations assumed that a crevice like geometry was already present. In other words, models presented to date were based on a macroscopic description of the problem. Little, however, is known about the early stages of coating disbondment before a macroscopic crevice develops. Thus, understanding the conditions leading to the onset of coating disbondment represent a significant need. In this work, the main variables leading to a loss in coating adhesion, which is the first step towards disbondment, were investigated. Improved understanding of how those factors affect chemical bonding between the steel substrate and the coating will promote the early detection of areas prone to SCC.

3 DEVELOPMENT OF A TEST METHODOLOGY TO CHARACTERIZE COATING DISBONDMENTS

3.1 Analysis of the critical variables

The use of a suitable methodology to rapidly study coating disbondment is critically important. Though many standardized test methods already exist, and were used in this project, it was crucial to validate that the test methodology used could reproduce in-service failure modes. The development of the test procedure was divided into different steps that included: 1) surface preparation, 2) adhesion strength measurements, 3) surface pH, 4) coating underside chemistry, and 5) anchor pattern. Below we describe the effects of the different variables on coating performance and the onset of disbondment.

3.1.1 Adhesion strength

When analyzing adhesion strength of coatings, three types of coating failure are possible: i) adhesive, ii) cohesive, and iii) substrate failure. Figure 1 illustrates the three different failure modes. In an adhesive failure the coating separates from the substrate cleanly and does not leave any coating attached. In a 100% cohesive failure, the coating breaks within itself and leaves a continuous layer of coating on the substrate even though the surface may have been completely removed. The third type of failure occurs when the substrate itself fails rather than the coating. This failure mode is common in concrete and it generally indicates the presence of a weakly adhere corrosion product. As explained by Mugner [9], if any type of failure is to be tolerated, a cohesive failure as shown in Figure 1b is preferred. A failure similar to the one shown in Figure 1b indicates that the bond between the steel substrate and the coatings remained intact and the coating still provides some protection. Changes in adhesion strength and failure mode are both indications of aging processes that could lead to an eventual coating failure.

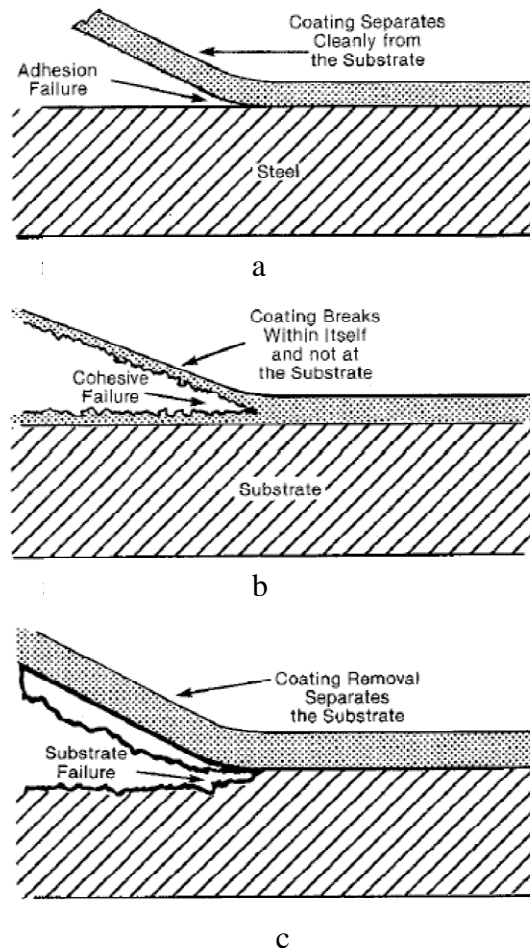


Figure 1. Types of coating failure: a) adhesive, b) cohesive, and c) Substrate failure.

The quantification of the adhesive strength of the coatings was performed using the ASTM D4541 “Pull-Off Strength of Coatings Using Portable Adhesion Testers” standard. This procedure was chosen over the scribe adhesion tests because it is quantitative and more reproducible [9]. Quantification of the adhesion strength is necessary to understand the effects of the different variables on the overall coating performance. Once cathodic disbondment has been initiated, the adhesive strength of the coating will decrease significantly. Thus, adhesive strength is the first parameter that could indicate the presence of disbondment.

The main limitation of this technique is the need for a strong two-part epoxy adhesive. This adhesive is used to attach a test dolly to the coating surface. In this regard, if the bond between the dolly and the coating is weaker than the bond between the coating and steel substrate, the test dolly would pull-off without measuring the coating bond strength.

Since the strength of the epoxy adhesive was extremely important, several commercial products were evaluated to determine which would give the highest strength. Only two products showed reasonable performance: Huntsman Araldite 8595A and Huntsman Araldite 2022. In both cases the maximum strength could reach approximately 6000 psi if properly cured. The main advantage of the Araldite 8595A over the 2022 is that the product is designed to cure on greasy or dusty surfaces, making it a better choice for field applications.

3.1.2 Surface pH

As described in the Introduction, one of the hypotheses for coating disbondment suggests that a highly alkaline environment, a consequence of CP, could weaken the bond between the coating and the steel substrate. Thus, measuring the surface pH can help in the determination of the coating failure mechanism. To accomplish this, the pH of the steel surface and the failed coating surface were measured using graduated pH strips on those regions where the coating failed after the pull-off adhesion test.

3.1.3 Coating underside chemistry

Understanding the environment that is generated inside a disbonded region is critical for establishing the actual degradation mechanism. In this regard, one of the most important variables to determine is the concentration of chloride ions at the surface. Using this information, the electro migration of ionic species inside a disbonded region could be inferred.

Several extraction and detection techniques exist. Nevertheless, as shown by Ruschau [9], the Bresle titration kit (described in the ISO 8502-2 standard) provided accurate results in an inexpensive and reproducible way. As a consequence, the Bresle kit has been implemented in this work.

In addition to chloride detection, the presence of surface rust was also examined and the composition of the oxide analyzed using X-ray diffraction (XRD). The coating under disbonded regions was evaluated using Fourier transformed infrared spectroscopy (IRS).

3.1.4 Anchor pattern

The surface roughness is another critical parameter that greatly influences adhesion. The surface roughness was measured using two different techniques: i) Testex Surface Profile and ii) Surface Laser Profilometry. The Testex kit is a rapid, field-friendly test that can estimate the surface roughness by measuring the peak height of the surface profile. However, this procedure is more qualitative in nature and the repetitiveness of the tests depends on the expertise of the person conducting the measurement. In contrast, extremely accurate surface roughness measurements can be obtained by surface laser profilometry (or equivalent interferometry techniques). In order

to conduct laser profilometry on the pipe samples, surface replicas are extracted using a Struers Repliset Kit. The replica was then analyzed in the laboratory.

3.1.5 Demonstration of the procedure on actual pipe sections

- 1) The first step consisted of documenting the pipe conditions including o'clock position, description of any visible damage, operational history of the pipe, and type of coating. In addition, soil conductivity and pH were measured (whenever possible this can be done in the lab by bringing soil samples in adequate containers).
- 2) After documenting the pipe history and conditions any completely disbonded coating is removed using a utility knife.
- 3) The next step consists in cleaning the surface to be analyzed. The cleaning procedure depends on the type of coating to be analyzed.

3.1) Fusion Bond Epoxy (FBE)

- i) Dirt/debris from surface is removed using water and a soft bristle brush or pad.
- ii) The surface is then gently abraded with a scratch pad.
- iii) The surface is subsequently degreased with an appropriate solvent (ethyl alcohol or acetone are preferred for most applications).

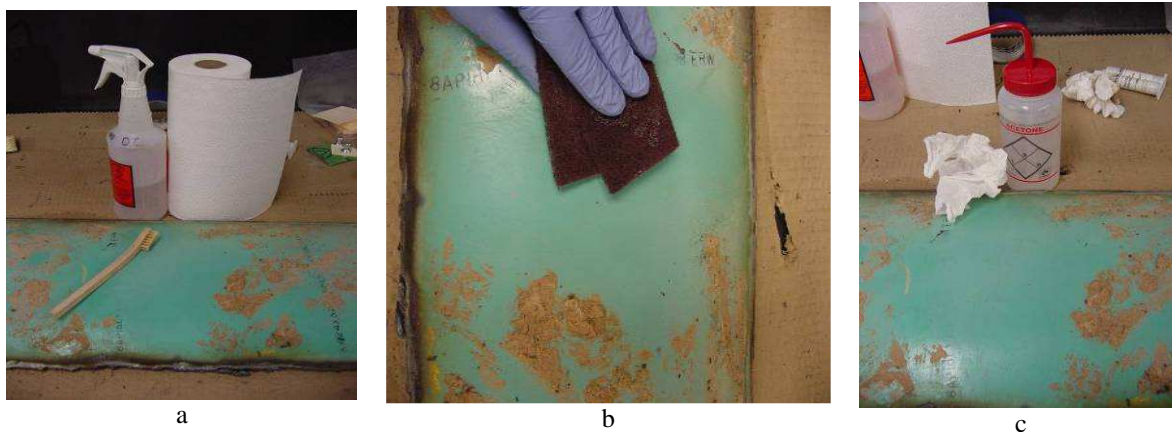


Figure 2. Cleaning steps for FBE coated pipes. a) step i, b) step ii, and c) step iii.

3.2) Coal Tar Enamel (CTE)

- i) Dirt/debris from surface is removed using water and a soft bristle brush or pad.
- ii) If present, external tape-wrap is first removed to expose the underlying coal tar layer.
- iii) The surface is then abraded with a wire brush.

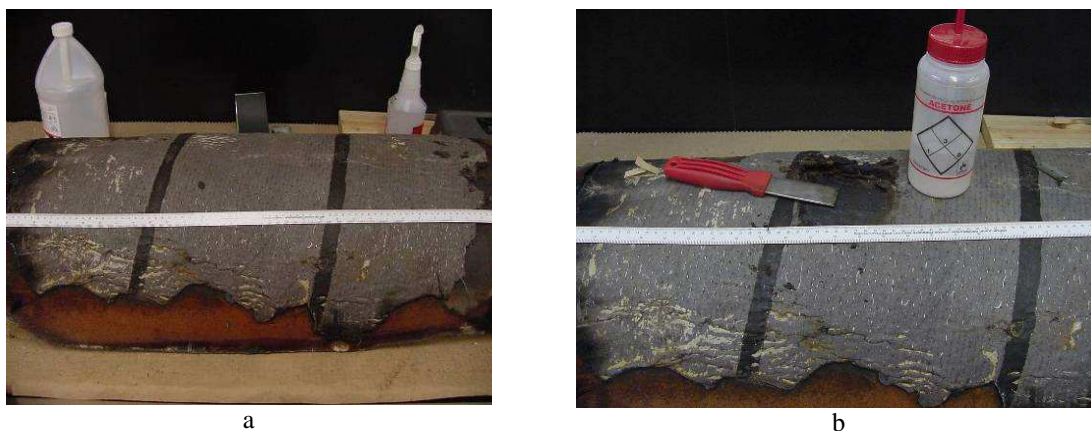


Figure 3. Cleaning procedures for coal tar enamel coated pipes. a) Step i, b) steps ii and iii.

- 4) Dollies are prepared according to the manufacturer procedures. An abrasive pad or sandpaper is used to remove any contamination from the surface of the dolly. Solvent (acetone) is used to degrease the base of the dollies to improve adhesion.
- 5) The two part epoxy-base adhesive (Huntman 8595 or 2022) is mixed according to the instructions provided by the manufacturer. The use of mixing nozzles is preferred.
- 6) The epoxy is then applied to the back side of the aluminum dollies (one at the time). Immediately after applying the epoxy, each dolly is positioned on the pipe surface. To obtain the highest adhesion strength from the epoxy adhesive, air bubbles have to be removed. This can be done by firmly pressing the dolly against the pipe surface until all the excess is displaced. Dollies must be secured to the pipe surface overnight using tape to facilitate curing of the epoxy.



Figure 4. Procedure to adhere the dolly to the pipe surface. a) Uniformly embed the base of the dolly with the epoxy-base adhesive and b) firmly press the dolly on the pipe surface until all the excess is displaced.

- 7) Once the two-part epoxy adhesive has properly cured, pull-off adhesion strength is determined following ASTM D7234 standard procedures. Before proceeding, it is important

to verify that the diameter of the dolly shown on the display matches the dolly that is being used.

- 8) After testing, dollies are clearly labeled and placed in containers matching the same identification convention.
- 9) Only for the areas where partial or complete adhesive failure was observed, chloride and pH characterization are conducted. The Bresle patch for swab extraction is prepared according to the ISO 8502-6 standard. The pH paper for pH assessment needs to be ready at the same time.
- 10) pH determination: The first step consists in immersing the swab in a beaker containing 2 ml of deionized water and gently dampening the surface of the pipe. The swab is then pressed against the pH paper indicator while attempting to minimize the amount of water remaining on the paper. The reading is entered immediately on the data sheet. After measuring the pH, the swab is placed in a clean empty glass container and the remaining water extracted by pressing the swab against the walls of the container.

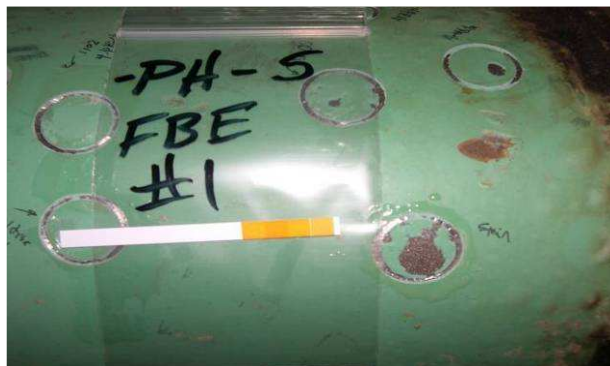


Figure 5. Example of pH determination procedure.

- 11) The swab extraction is repeated one more time without measuring pH.
- 12) Chloride content: To determine chloride content, a Bresle detection kit is recommended. The procedure described in the ISO 8502-10 standard is followed and the results recorded on the data sheet.

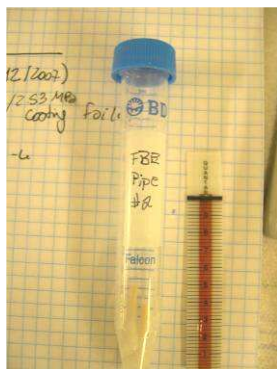


Figure 6. Bresle kit for chloride determination.

- 13) After pH and Chloride detection the anchor pattern has to be determined. To do so, the Struers Repliset epoxy kit has to be applied on the pipe surface and proper curing time allowed (approximately 30 minutes). After curing, the epoxy needs to be peeled off and placed on a glass slide in a bag for further analysis and subsequent imaging.

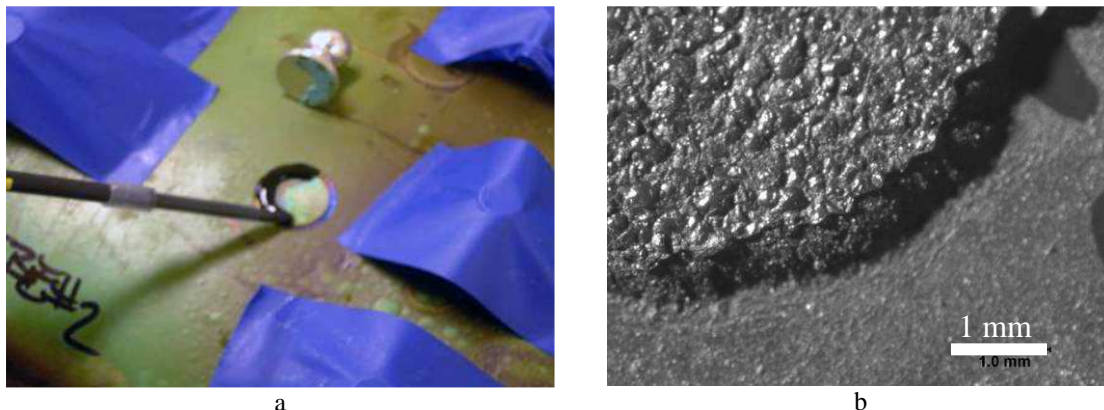


Figure 7. Application of Struers Repliset Kit. a) Application of the resin on a pipe surface using the application gun and the mixing nozzles provided by the manufacturer, and b) optical stereo-micrograph of the replicated surface showing the anchor pattern of the pipe.

- 14) The Testex surface profile gauge is used to get a profile measurement. The procedure used was as follows: i) the initial thickness of the film is measured prior to use with the snap gauge, ii) the film is applied on the uncoated surface. Then, the round cut out portion of the “Press O Film” is rubbed over using the burnishing tool provided with the kit. The film will become uniformly darker when replicated. The film is then placed between the anvils of the snap gauge and the measurement recorded. Finally the profile, in mils, is obtained by subtracting the initial thickness of the film from the profile measurement.

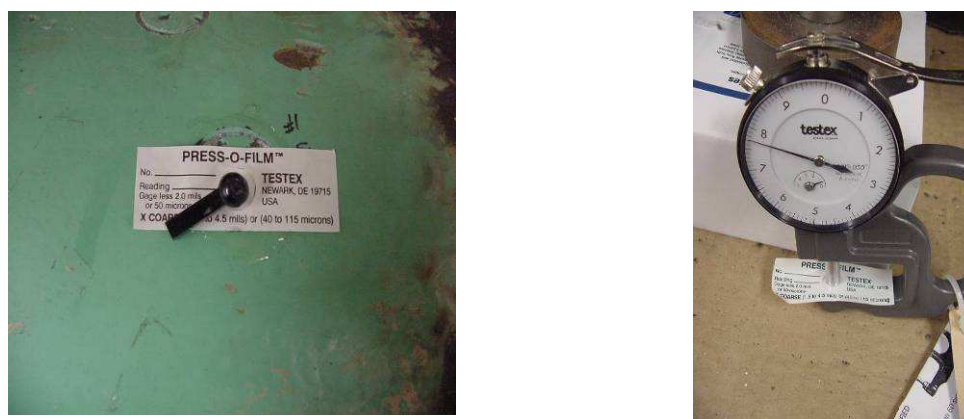


Figure 8. Use of the Testex Surface Profile gauge to obtain surface roughness.

- 15) If evident signs of surface oxidation were observed, samples of surface rust are brought to the lab for analysis.

4 CHARACTERIZATION OF AVAILABLE AND ADDITIONAL PIPE SECTIONS

An evaluation of existing coated pipe sections in the DNV Columbus inventory was conducted. FBE, coal tar enamel (CTE), and reinforced coal tar enamel (RCTE) coated pipes were selected. FBE sections were obtained from pipes in service for about 20 years, whereas coal tar samples represented pipes often more than 50 years old. Pipe sections were analyzed according to the procedures described in Section 3 above.

Based on an initial survey of DNV Columbus inventory, it was found that no available pipe sections showing visible signs of coating disbondment were available. The main reason for this is that the coatings were usually removed from the affected area during any failure investigation conducted in the field. In many cases the removal of the coating was done prior to shipping the pipe segment for additional study and analysis in the laboratory. However, the absence of visible signs of disbondment was not necessarily an indication that the coated pipes were free of defects. Results from examining a series of pipe segments are summarized in the tables below.



Figure 9. Example of Pull-Off adhesion strength dollies curing on a FBE-coated pipe.

Table 1. Results of Pull Off Adhesion Tests on Pipe ID FBE # 3

Dolly #	Dolly Size	Location	Strength	Epoxy Type	Failure Type
1	14mm	Flat Surface	1735psi	Huntsman 8595	No Failure
2	20mm	Flat Surface	3302psi	Huntsman 8595	No Failure
3	14mm	Flat Surface	3620psi	Huntsman 8595	No Failure
4	14mm	Flat Surface	2142psi	Huntsman 8595	No Failure
5	20mm	Flat Surface	6632psi	Huntsman 8595	No Failure
6	20mm	Flat Surface	2680psi	Huntsman 8595	No Failure
7	14mm	Flat Surface	3388psi	Huntsman 8595	No Failure
8	14mm	Flat Surface	3028psi	Huntsman 8595	No Failure
9	14mm	Flat Surface	3734psi	Huntsman 8595	No Failure
10	20mm	Flat Surface	2518psi	Huntsman 8595	No Failure

Table 2. Results of Pull Off Adhesion Tests on Pipe ID FBE # 3

Dolly #	Dolly Size	Location	Strength	Epoxy Type	Failure Type
1	14mm	Flat Surface	2376psi	Huntsman 2022	Coating Failure
2	14mm	Flat Surface	3497psi	Huntsman 2022	Could not pull off
3	14mm	Flat Surface	4144psi	Huntsman 2022	No Failure
4	14mm	Flat Surface	2768psi	Huntsman 2022	No Failure
5	14mm	Flat Surface	3618psi	Huntsman 2022	No Failure
6	14mm	Flat Surface	2124psi	Huntsman 2022	No Failure
7	14mm	Flat Surface	3510psi	Huntsman 2022	Could not pull off
8	14mm	Flat Surface	3820psi	Huntsman 2022	No Failure
9	14mm	Flat Surface	4218psi	Huntsman 2022	No Failure
10	14mm	Flat Surface	1500psi	Huntsman 2022	No Failure

Table 3. Results of Pull Off Adhesion Tests on Pipe ID FBE # 11

Dolly #	Dolly Size	Location	Strength	Epoxy Type	Failure Type
1	14mm	Flat Surface	1131psi	8595	Adhesion Failure
2	14mm	Flat Surface	2892psi	8595	Adhesion Failure
3	14mm	Flat Surface	2436psi	8595	Adhesion Failure
4	14mm	Flat Surface	2176psi	8595	Adhesion Failure
5	14mm	Flat Surface	1272psi	8595	Adhesion Failure
6	14mm	Flat Surface	1558psi	2022	Adhesion Failure
7	14mm	Flat Surface	3336psi	2022	Adhesion Failure
8	14mm	Flat Surface	3092psi	2022	Adhesion Failure
9	14mm	Flat Surface	2118psi	2022	Adhesion Failure
10	14mm	Flat Surface	4088psi	2022	Adhesion Failure
11	14mm	Flat Surface	1466psi	2022	Coating Failure
12	14mm	Flat Surface	2454psi	2022	Adhesion Failure

Table 4. Results of Pull Off Adhesion Tests on Pipe ID FBE # 12.

Dolly #	Dolly Size	Location	Strength	Epoxy Type	Dolly #
1	14mm	Flat Surface	1284psi	2022	Adhesion Failure
2	14mm	Flat Surface	2720psi	2022	Adhesion Failure
3	14mm	Flat Surface	2562psi	2022	Adhesion Failure
4	14mm	Flat Surface	2364psi	2022	Adhesion Failure
5	14mm	Flat Surface	2576psi	2022	Adhesion Failure
6	14mm	Flat Surface	3278psi	2022	Adhesion Failure
7	14mm	Flat Surface	2982psi	2022	Adhesion Failure
8	14mm	Flat Surface	952psi	2022	Adhesion Failure
9	14mm	Flat Surface	1344psi	2022	Adhesion Failure
10	14mm	Flat Surface	2308psi	8595	Adhesion Failure
11	14mm	Flat Surface	1916psi	8595	Coating Failure
12	14mm	Flat Surface	3256psi	8595	Adhesion Failure
13	14mm	Flat Surface	972psi	8595	Adhesion Failure
14	14mm	Flat Surface	1776psi	8595	Adhesion Failure
15	14mm	Flat Surface	1806psi	8595	Adhesion Failure

Table 5: Characterization of CTE pipe # 1. PSI Indicates adhesion strength in PSI.

Dolly Number (ID)	PSI	Failure Type	Chemistry	
			pH	Cl- (ppm)
1	386	cohesive	XXX	XXX
2	497	cohesive	XXX	XXX
3	488	cohesive	XXX	XXX
4	379	cohesive	XXX	XXX
5	426	cohesive	XXX	XXX
6	379	cohesive	XXX	XXX
7	331	cohesive	XXX	XXX
8	261	cohesive	XXX	XXX
9	212	cohesive	XXX	XXX
1	394	cohesive	XXX	XXX
2	661	cohesive	XXX	XXX
3	664	cohesive	XXX	XXX
4	197	cohesive	XXX	XXX
5	652	cohesive	XXX	XXX
6	115	cohesive	XXX	XXX
7	683	cohesive	XXX	XXX
8	191	cohesive	XXX	XXX
9	465	cohesive	XXX	XXX

Table 6: Characterization of CTE pipe # 2. PSI Indicates adhesion strength in PSI.

Dolly Number (ID)	Epoxy	PSI	Failure Type	Chemistry	
				pH	Cl ⁻ (ppm)
1	2022	XXX	XXXXX	XXX	XXX
2	2022	148	cohesive	XXX	XXX
3	2022	295	cohesive	XXX	XXX
4	2022	177	cohesive	XXX	XXX
5	2022	308	cohesive	XXX	XXX
6	2022	291	cohesive	XXX	XXX
7	2022	284	cohesive	XXX	XXX
8	2022	337	cohesive	XXX	XXX
9	2022	XXX	XXXXX	XXX	XXX
10	2022	XXX	XXXXX	XXX	XXX
1	8595	474	cohesive	XXX	XXX
2	8595	551	cohesive	XXX	XXX
3	8595	394	cohesive	XXX	XXX
4	8595	375	cohesive	XXX	XXX
5	8595	481	cohesive	XXX	XXX
6	8595	303	cohesive	XXX	XXX
7	8595	385	cohesive	XXX	XXX
8	8595	322	cohesive	XXX	XXX
9	8595	XXX	XXXXX	XXX	XXX
10	8595	260	cohesive	XXX	XXX

Tables 1-4 summarize the results obtained for FBE pipe samples and Tables 5 and 6 the results of CTE sections. Additional CTE and RCTE pipe sections were tested all showing identical results to the ones presented in Tables 5 and 6.

As can be seen from Tables 1-4 the variability of the adhesion strength was significant. This was due to differences in curing of the two-part epoxy adhesive used to attach the dollies to the pipe. Nevertheless, properly cured, defect-free FBE coatings showed adhesion strength values greater than 4000 psi, and in some cases greater than 6000 psi. These adhesion strengths are above the adhesion strength of most commercial adhesives and as a result “adhesion failures” (the epoxy bond between the dolly and the coating rather than the bond between the coating and the pipe failed) were noted. As shown in Tables 1-4, three of the FBE coatings did fail at a single location on each of the three different pipes. Surface characterization was conducted on those areas as described by the standardized technique in Section 3 previously. Results from analyzing the three failure locations are summarized on Table 7. According to these results, coating failure occurred on the order of 1400 – 2400 psi. There were no signs of chloride contamination and the pH was near neutral.

Table 7. Results of Pull Off Adhesion Tests on Pipe ID FBE # 12.

Pipe ID	Dolly #	Failure Strength	pH	Chloride
FBE# 3	1	2376psi	6	<31ppm
FBE # 11	11	1466psi	6-7	<31ppm
FBE # 12	11	1916psi	6-7	<31ppm

In contrast, all the tests performed on CTE and RCTE coatings showed cohesive failure with a maximum strength that varied from about 200 psi to 600 psi. A typical cohesive failure is shown in Figure 10. Because most of the available FBE sections did not show any signs of deterioration, as evidenced by the extremely high adhesion strength values, it was decided to intentionally damage the coatings to assess the conditions leading to such superior adhesion (Figure 11). FBE coated sections were heated with a methane torch for a few minutes until blistering was observed on the surface of the pipe. Dollies were attached on areas showing evident signs of blistering. The entire standardized procedure was then followed. Typical results are summarized below.



Figure 10. Typical appearance of coal tar coating showing cohesive failure.



Figure 11. Typical appearance of an intentionally blistered FBE coated pipe.

Table 8. Test results for pipe FBE #2 - Blistered.

Dolly ID	Location	Coating Failure	PSI	pH	Cl	Testex Profile
Dolly#1	Blister	yes	368	5-6	<31ppm	2.7mils
Dolly#4	Blister	yes	104	5	<31ppm	3.1mils
Dolly#7	Blister	yes	768	5-6	<31ppm	2.7mils
Dolly#8	Blister	yes	0	6	<31ppm	4.2mils
Dolly#10	Blister	½ removal	368	5-6	<31ppm	2.8

As can be observed from Table 8, the surface under defect free FBE showed no signs of chloride contamination as evidenced by the titration analysis. The pH of those areas was between 5 and 6, and the surface profile corresponded to a white sand blast finish. The typical roughness was measure to be approximately 2-3 mils.

In contrast to the FBE case, heating of the pipe surface melted the coal tar layer producing no blistering. Likewise, as shown in Table 5 and Table 6, CTE and RCTE sections always produced cohesive failures, making further surface characterization impossible. Thus, consecutive pull-off adhesion tests were conducted on the same locations in an attempt to eventually induce adhesive failure of the coating. Cohesive failures were observed even after pulling 3-4 layers of the CTE coatings. There always seemed to be a thin coal tar film adhered to the surface, which is an indication of a well performing coating. As a consequence, no surface analysis could be performed on coal tar enamel sections after pull-off adhesion tests.

To overcome this problem, areas of the coal tar samples were impacted by a hammer to remove small fragments of the coating. Surface chemistry analysis were conducted under those regions and compared against results of defect-free FBE coatings. Table 9 summarizes the chemistry under coal tar coatings. Results shown in Table 9 are similar to the findings presented for the intact FBE coatings. The pH was about neutral and the surface chloride content below 31 ppm.

Table 9. Surface under coating chemistry on Coal Tar samples

Pipe ID	pH				Chloride			
	pH#1	pH#2	pH#3	pH#4	CL#1	CL#2	CL#3	CL#4
CT#5	5-6	5	5-6	5	<31ppm	<31ppm	<31ppm	<31ppm
CT#2	5-6	6	5	5	<31ppm	<31ppm	<31ppm	<31ppm
CT#3	5	5	5-6	5	<31ppm	<31ppm	<31ppm	<31ppm
CT#4	5	5	5		<31ppm	<31ppm	<31ppm	-
RCT#2	5	5	5	5	<31ppm	<31ppm	<31ppm	<31ppm
RCT#1	5	5	6-7	5	<31ppm	<31ppm	<31ppm	<31ppm

4.1 Cathodic Disbondment Tests (CDT) on New and Aged Pipe Sections

Since the characterization of aged FBE and CTE pipe sections indicated no signs of coating disbondment and the surface condition of the steel prior to coating application was unknown, it

was necessary to develop a series of laboratory scale procedures to study the initiation of coating disbondment. The tests were divided in three: i) CDT on new pipe sections, ii) CDT on aged pipe sections, and iii) CDT on flat coupons. In this section the results of this investigation are presented and discussed in detail.

4.1.1 CDT on new pipe section and coupons

4.1.1.1 New Pipe Sections

The objective of this aspect of the investigation was to quantify the effects of surface finishing and cleanliness on the performance of FBE coatings under CP. Four new pipe sections of about 70 cm in length and 25 cm in diameter with a white-sand-blast finish were obtained from LaBarge Pipe & Steel Co. Four different surface conditions were then produced: 1) as-received (no contamination), 2) chloride contaminated, 3) flash rust, and 4) mud and grease contamination.

The sample in the as-received condition was cleaned using a mixture of deionized (DI) water and an alkaline detergent (Liquinox), followed by final DI water rinse. The pipe section was then dried using compressed nitrogen and placed in a sealed storage bag to minimize oxidation. Chloride contamination was achieved by uniformly spraying a 0.5 M NaCl solution over a clean pipe section that was heated above 100 °C. In this way, the solution evaporated immediately upon contacting the pipe surface leaving a thin chloride-rich layer. The flash rust surface contamination was obtained by placing a clean pipe section in a furnace at 60 °C and 100% relative humidity (RH) for 7 days. Finally, mud and grease contamination was produced by first leaving fingerprints on the surface of a clean pipe and then dipping the section in a container filled with a suspension of DI water and Dublin soil. All sections were stored in a sealed container. After the surface pre-treatment was completed samples were sent to Custom Pipe Coating, Inc for FBE application.

Coated samples were cut into two equal segments and characterized prior to the CDT following the procedure described in Section 3. As shown in Figure 12, adhesion strength was highest for the sample in the as-received condition. Adhesion strength reached, on average, approximately 4000 psi with no coating failure. Adhesion strength decreased for the other three conditions with chloride contamination showing the lowest values. All the samples subject to surface pre-treatments showed some degree of coating failure. Oxide contamination was the best performing treatment.

Table 10 shows the results of the surface chemistry characterization conducted on the pipe sections before CDT. In this case surface characterization was conducted using ion exchange chromatography (IEC). As observed in Table 10, there was some variability in the amount of chloride detected by IEC, which reflects the variability on the amount of chloride recovered during swab extraction. Surface chloride varied from 33.40 to 127 ppm. Virtually no chloride

was found in the oxide and mud-grease samples. Levels of fluoride, bromide, phosphate, and sulfate were almost negligible.

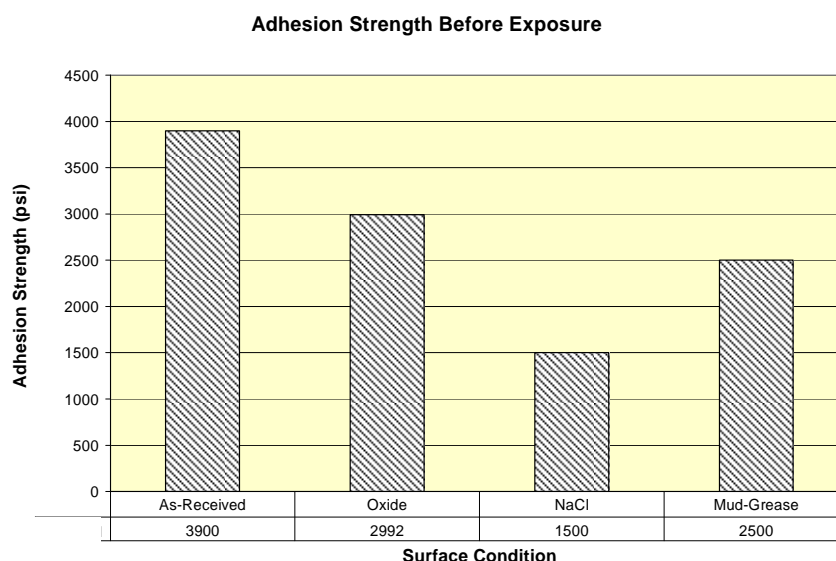


Figure 12. Adhesion strength before exposure as a function of surface treatment.

Table 10. Surface characterization via IEC before exposure.

Sample ID	Location	Analyte Composition (ppm)						
		Fluoride	Chloride	Nitrite	Bromide	Nitrate	Phosphate	Sulfate
Oxide B	3 o'clock	0.76	2.04	ND	ND	ND	ND	ND
NaCl A	12 o'clock	0.25	126.00	ND	ND	ND	ND	5.23
NaCl A	3 o'clock	ND	70.30	ND	ND	ND	ND	2.89
NaCl A	9 o'clock	ND	127.00	ND	ND	ND	ND	3.52
NaCl B	12 o'clock	ND	50.00	ND	ND	ND	ND	0.40
NaCl B	3 o'clock	ND	32.40	ND	ND	0.26	ND	1.97
NaCl B	9 o'clock	ND	46.60	ND	ND	ND	ND	2.47
Mud & Grease A	3 o'clock	ND	1.73	0.31	ND	ND	ND	0.38
Mud & Grease A	9 o'clock	ND	1.54	0.30	ND	0.33	3.44	ND
Mud & Grease B	12 o'clock	1.38	3.23	ND	ND	ND	ND	ND
Mud & Grease B	3 o'clock	ND	2.67	ND	ND	ND	1.39	0.88

To induce coating disbondments, acrylic cells were attached to the available pipe samples. A small defect was introduced in the coating in order to expose the bare pipe surface. The exposed area was approximately 0.4 cm². The acrylic cells were filled with Dublin soil. The resistivity of the soil was adjusted to 900 to 100 kΩ-cm using a solution containing 0.5 M NaCl. An Mg anode was electrically connected to the pipe in order to induce some level of cathodic protection. Tests were conducted at room temperature. The experimental setup is summarized in Figure 13 and

Figure 14. The *on* and instant-*off* potentials were monitored twice a week. The duration of the tests was 55 days. A chemical analysis of the soil used for these tests is shown in Table 11. The chemical analysis was performed using colorimetric and titration methods.

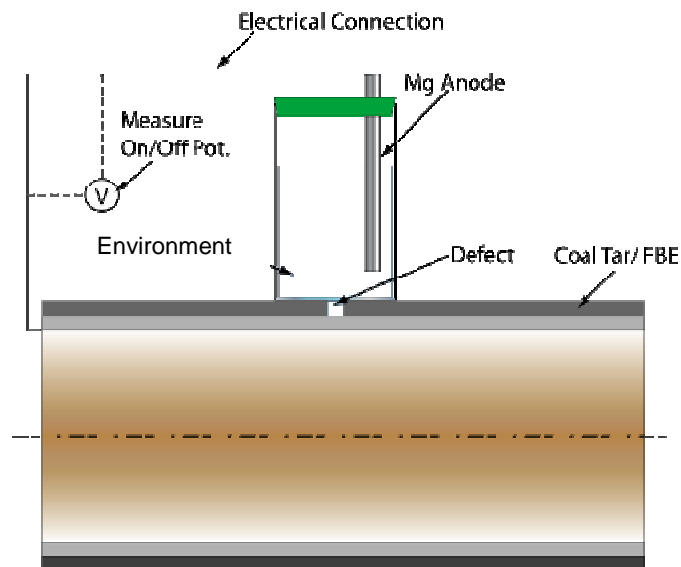


Figure 13. Schematic representation of the CDT setup.

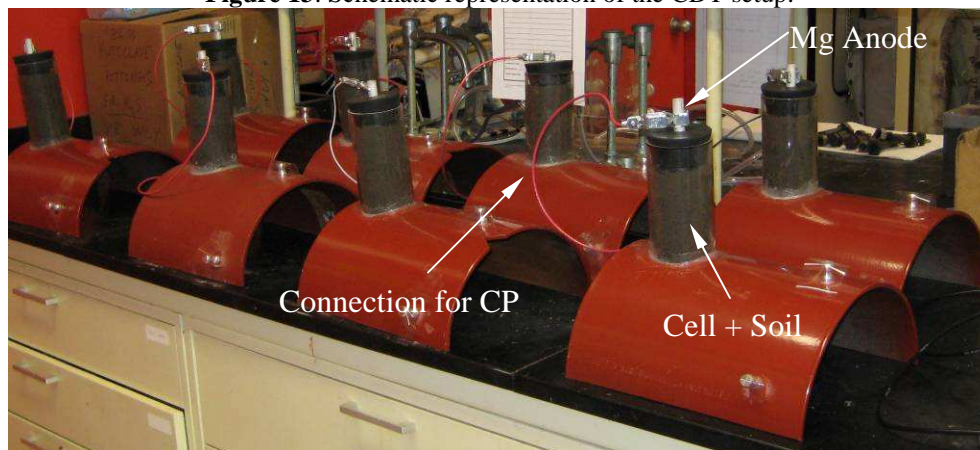


Figure 14. Picture of the 8 pipe sections used for this investigation.

Table 11. Chemical analysis of the soil before testing.

Field ID	Soluble Cations mg/kg		Soluble Anions, mg/kg							pH Soil	Total Acidity mg CaCO ₃ /kg	Total alkalinity mg CaCO ₃ /Kg	Moisture Content %	Resistivity Ohm-cm
	Ca ²⁺	Mg ²⁺	NO ₂ ⁻	NO ₃ ⁻	Cl ⁻	SO ₄ ⁻	S ²⁻	CO ₃ ²⁻	CO ₃ ⁻					
100g of Soil in 500 ml H ₂ O	318.8	64.4	0.157	4.184	90.1	376.36	<24	254.5	517.5	8.11	0	424.2	24.56	2300

Results of *on* and instant-*off* potentials are shown in Figure 15. As shown in Figure 15 the *on* potentials were more negative than the -0.95V criterion for the duration of the test. However, the instant-*off* potentials were lower than the -0.95 V instant-*off* criterion and very scattered during the test. Nevertheless, due to the high *on* potentials, the exposed defects were polarized in the region where hydrogen evolution is expected.

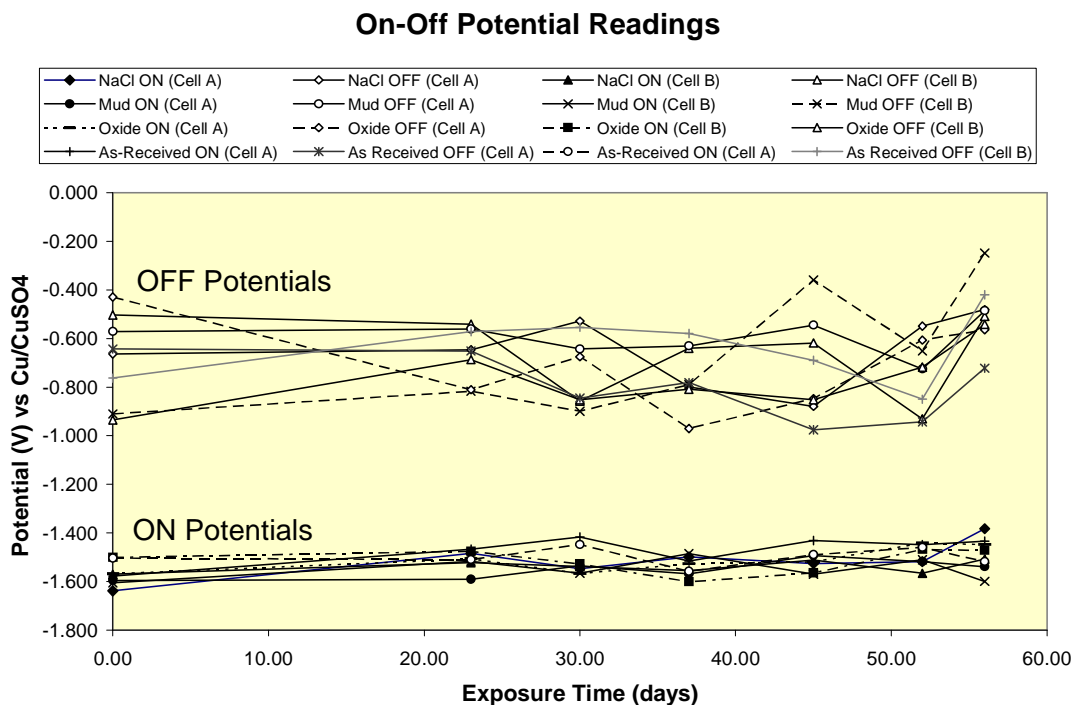


Figure 15. On-off potential readings during the 55 days of exposure.

After exposure the acrylic cells were removed and the surface of the pipe sections prepared for pull-off adhesion testing. Dollies were placed at incremental distances from the original defect in a cross-like pattern. The distance between consecutive dollies was approximately 5 cm. Figure 16 illustrates the post-exposure adhesion experimental setup assuming that macroscopic disbondment occurred.

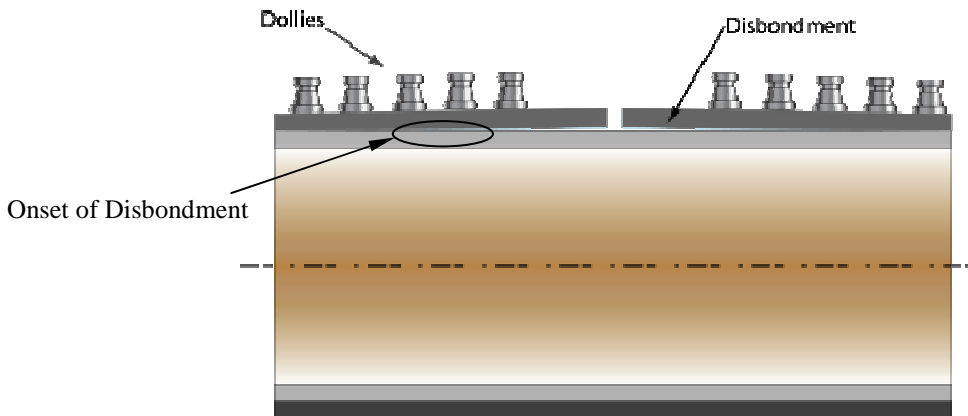
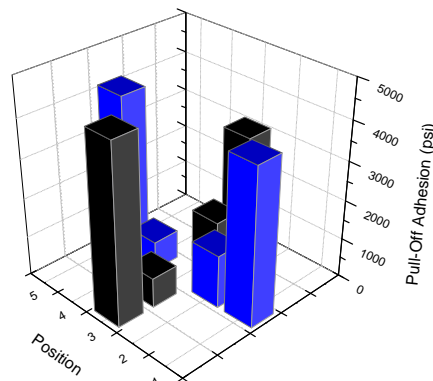


Figure 16. Post-exposure experimental setup showing the location of the dollies. Pull-off adhesion tests were conducted at incremental distances from the defect.

Results of the pull-off adhesion tests are shown below. The bars in the charts shown in Figure 17 to Figure 24 represent the adhesion strength measured at a given position. The defect is located at the center of the x and y axes. Corresponding photographs of the failed areas are also shown. Table 12 summarizes the average surface chemistry results. Chloride and pH measurements were taken from both the steel surface and the back of the failed FBE coating as illustrated in Figure 25.

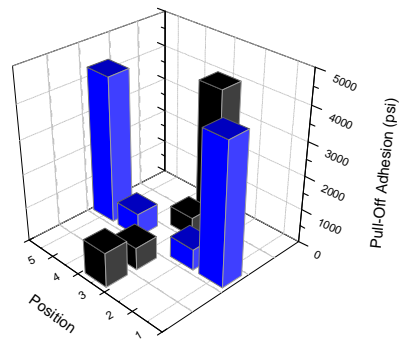


a



b

Figure 17. As-received Section #A: a) adhesion strength and b) surface after pull-off test

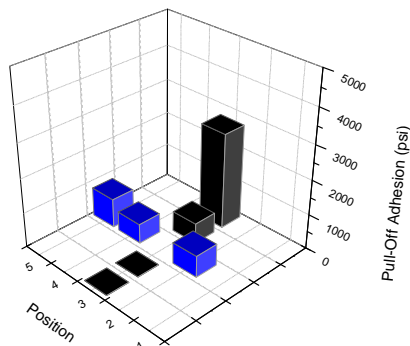


a



b

Figure 18. As-received Section #B: a) adhesion strength and b) surface after pull-off test



a



b

Figure 19. Chloride Contamination Section #A: a) adhesion strength and b) surface after pull-off test

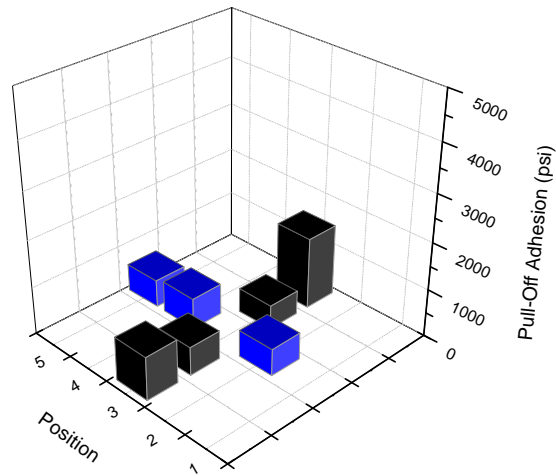


Figure 20. . Chloride Contamination Section #B: adhesion strength

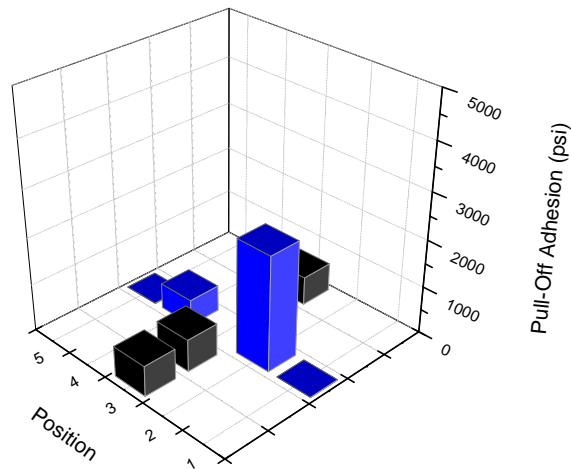
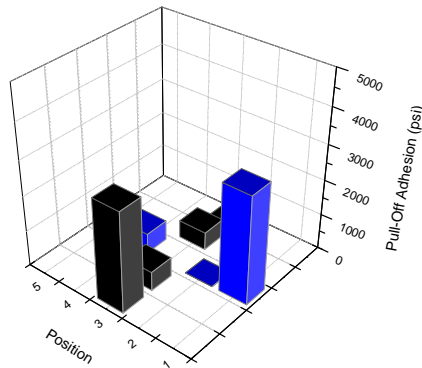


Figure 21. Oxide Contamination Section #A: adhesion strength.

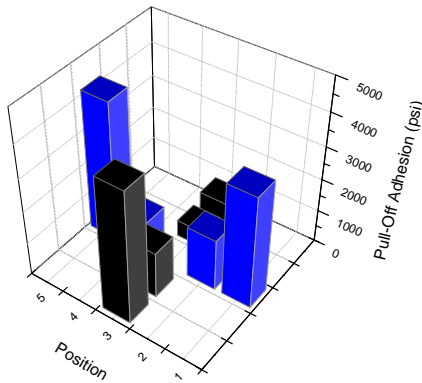


a



b

Figure 22. Oxide Contamination Section #B: a) adhesion strength and b) surface after pull-off test

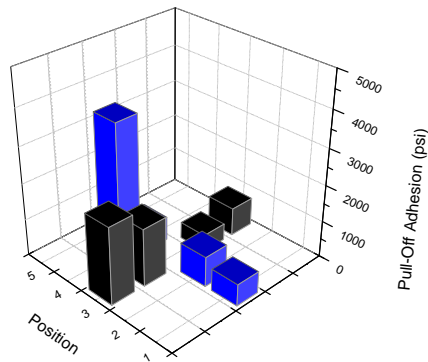


a



b

Figure 23. Mud/Grease Contamination Section #A: a) adhesion strength and b) surface after pull-off test



a



b

Figure 24. Mud/Grease Contamination Section #A: a) adhesion strength and b) surface after pull-off test

Table 12. Average chemistry measurements as a function of surface treatment

Surface Condition	Surface Chloride Content (ppm)	Surface Chloride on FBE (ppm)	Surface pH	Surface pH on FBE
As-Received	<31	<31	5	4-5
NaCl	44-57	50-97	4-5	5-6
Oxide	<31	<31	5-6	5
Mud-Grease	<31	<31	5	4-6

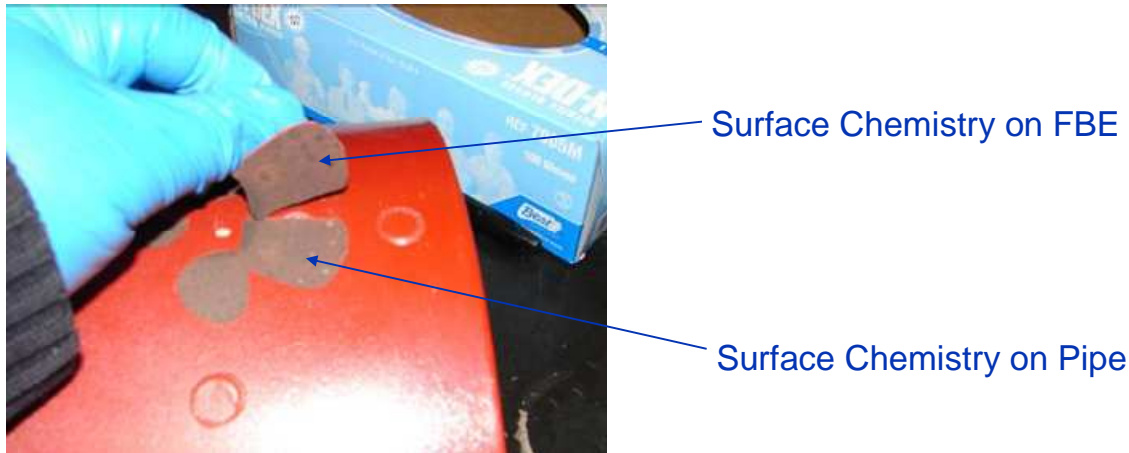


Figure 25. Surface chemistry was measured on both the steel substrate and the back of the failed FBE coating.

As seen in Figure 17 and Figure 18, the adhesion strength of the coating near the defect decreased from about 4000 psi to less than 1800 psi after exposure. The dollies placed in the proximities of the defect were included within the area that was covered by the acrylic cell during the CDT. However, as seen in Figure 18, coating failure also occurred outside the exposure region. That is, the failure zone extended beyond the actual exposed area for the CDT. This observation combined with the fact that no coating failure occurred on the tests before exposure seems to indicate that the extension of the coating damage was not confined to the region exposed to the soil environment.

To determine the actual extent of the damage, the coating was gently scraped off using a utility knife. All the coating that was easily peeled with the knife was removed. The surface pH was measured at the defect and, at least, at four other locations to determine if a possible gradient in pH along the failed surface existed. Results are shown in Figure 26. As seen in Figure 26, the pH was approximately 10-11 in the region surrounding the defect; but was nearly neutral everywhere else. Figure 27 shows the results of a control test performed on the same pipe away from the affected area. The test was conducted to determine whether the large extent of coating failure was somehow related to defective or poor coating application. As seen in Figure 27, peeling of the coating was difficult and confined to the area near the CDT exposure area. Although a defective coating due to application errors should not be completely ruled out, these results seem to confirm that the disbonded region extending outside the area exposed to the CDT was likely caused by the CDT experiment itself. Possible explanations for this observation will be discussed later.

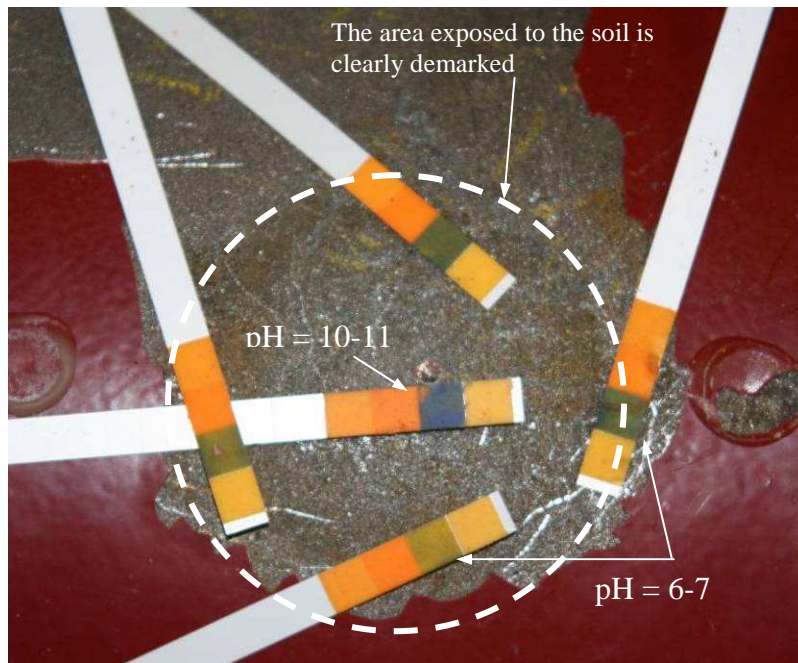


Figure 26. Extent of the attack and pH indication after test on as-received section B

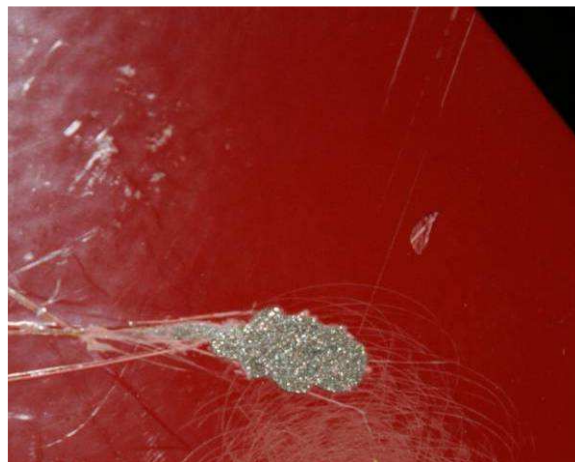


Figure 27. Control test showing that away from the damaged area peeling of the coating was not possible, indicating good adhesion.

As seen in Figure 19 and Figure 20, the adhesion strength measured on the samples that were pre-treated with chloride was the lowest. No significant changes were found in the surface chloride measurements after testing and the pH at the surface of the pipe and at the failed coating were close to neutral. After pull-off adhesion measurements, the coating was gently scraped with a utility knife and the pH measured at various locations. As shown in Figure 28, almost the entire coating was removed by the knife. In this case, however, this was not necessarily caused by the CDT since adhesion was affected by the pre-treatment as evidenced by the initial low strengths

measured before CDT testing. The objective of the chloride pre-treatment was to evaluate how the presence of chloride affects ionic migration. The surface pH was 6-7 everywhere but at the proximities of the defect, where the pH reached 10-11. The back side of the failed coating near the defect also showed a pH of 10-11.



Figure 28. Extent of the attack and pH indication after test on chloride pre-treated pipe.

Similar results were obtained for mud/grease and oxide pre-treatments. In both cases adhesion strength was in between the as-received and chloride cases as illustrated in Figure 21 to Figure 24. Measurements of surface pH and chloride content were also in line with previous findings. Removal of the coatings by scraping revealed that the pH increased to values near 10-11 only at locations near the defects. Removal of the coatings was almost complete. As in the chloride pre-treatment case, this was not necessarily caused by the CDT but by the lower adhesion strength of the FBE coating as a consequence of having a contaminated surface prior to coating application.

4.1.2 CDT on aged pipe sections

CDT was also conducted on aged FBE and coal tar coated pipes available at DNV Columbus. The objective of this investigation was to induce coating disbondments so that the evolution of the chemistry under the affected area could be analyzed and compared with the laboratory generated sample results.

For CDT on aged pipe sections, two types of electrolytes were used: i) 0.5 M NaCl and ii) Dublin soil. In contrast to the previous tests, the initial surface condition was unknown. Since the pipe sections were stored outdoors, the temperature of the tests was not controlled. Mg anodes were used as before to induce cathodic protection.

A total of 8 pipe samples were tested: 2 FBE, 4 CT, and 2 RCT with average service lives greater than 15 years. Two cells (one with NaCl solution and one with soil) were attached to each pipe sample. In NaCl, gas (hydrogen) evolution occurred immediately after connecting the steel pipe to the Mg anode, as shown in Figure 29.

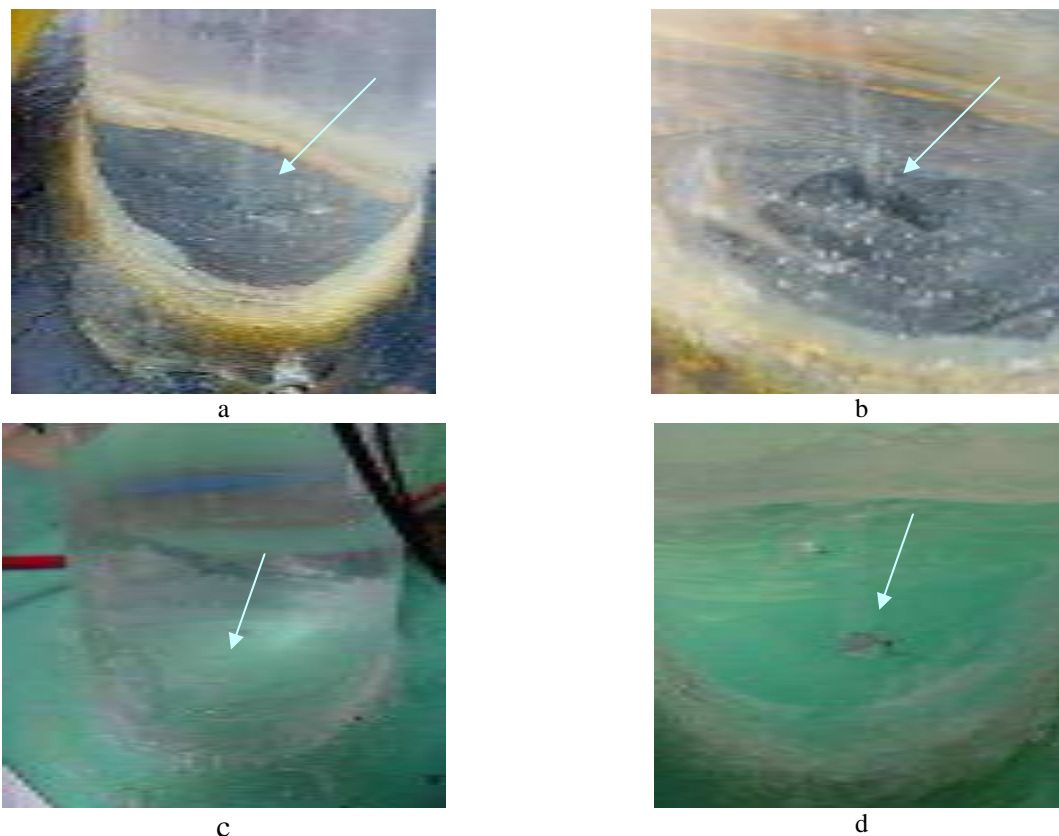


Figure 29. Gas (hydrogen) evolution is witnessed by the formation of bubbles at the holiday after connecting the steel substrate with the Mg sacrificial anode for Coal Tar in a) and b) and on FBE in c) and d).

On and instant-off potentials readings were taken periodically. Results are shown in Figure 30. For NaCl and soil, the *on* potential averaged about -1.5 V vs Standard Calomel Electrode (SCE). In NaCl, the instant-off potential gave, on average, -0.75 V vs SCE. The average difference between the *on* and the instant-off potential gave a polarization of about 750 mV. The instant-off potential in soil was very erratic and averaged approximately 700 mV, giving a difference of -800 mV with respect to the *on* potential.

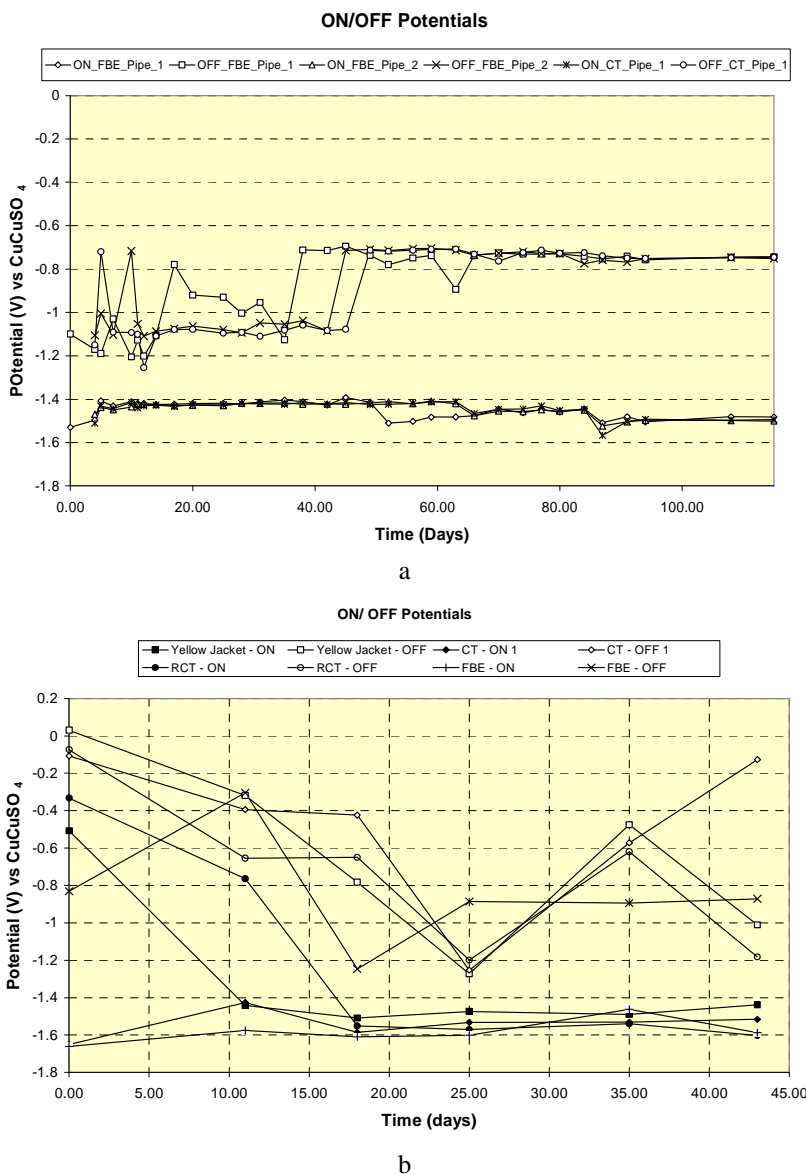


Figure 30. On and instant off potential readings: a) in 0.5 M NaCl and b) Dublin soil.

The duration of the test in 0.5 M NaCl was 120 days and the duration of the tests in soil was 45 days. After testing the cells were removed and the pipe sections characterized following the standard procedure described in Task 1. Results are shown below. Results are sorted by environment and coating type. In Tables 12 to 19 the column labeled Epoxy refers to the type of adhesive used to attach the dollies to the pipe surface. A selected number of samples were sent for ISC analysis. Results are shown in Table 21 and Table 22.

Table 13. Adhesion strength and surface characterization after CDT: FBE in 0.5M NaCl

Dolly Number (ID)	Epoxy	Dolly Size	Strength	Failure Type	Chemistry	
	Type	mm	PSI		pH	Cl- (ppm)
H1	2202	14	3900	epoxy	XXX	XXX
H2	2202	14	1320	adhesive	5 to 6	<31 (0Q)
H3	2202	14	397	adhesive	5 to 6	<31 (0Q)
H4	2202	14	4688	epoxy	XXX	XXX
V1	2202	14	3748	epoxy	XXX	XXX
V2	2202	14	2136	partial adhesive	5 to 6	<31 (0Q)
V3	2202	14	468	partial adhesive	5 to 6	<31 (0Q)
V4	2202	14	3878	epoxy	XXX	XXX

Table 14. Adhesion strength and surface characterization after CDT: CT #1 in 0.5M NaCl

Dolly Number (ID)	Epoxy	Dolly Size (mm)	PSI	Failure Type	Chemistry	
					pH	Cl- (ppm)
H1	8595	20	456	adhesive	5	<31 (0.1Q)
H2	8595	20	692	adhesive	6	0 (0Q)
V1	8595	20	476	adhesive	5.5	0 (0Q)
V2	8595	20	692	adhesive	6	<31 (0.4Q)
H1	8595	50	220	cohesive	XXX	XXX
H2	8595	50	161	cohesive	XXX	XXX
V1	8595	50	331	cohesive	XXX	XXX

Table 15. Adhesion strength and surface characterization after CDT: CT #2 in 0.5M NaCl

Dolly Number (ID)	Epoxy	Dolly Size (mm)	PSI	Failure Type	Chemistry	
					pH	Cl- (ppm)
H1	2202	14	724	cohesive	XXX	XXX
H2	2202	14	XXX	XXXXXXXX	XXX	XXX
H3	2202	14	376	cohesive	XXX	XXX
H4	2202	14	XXX	XXXXXXXX	XXX	XXX
V1	2202	14	338	cohesive	XXX	XXX
V2	2202	14	XXX	XXXXXXXX	XXX	XXX
V3	2202	14	572	cohesive	XXX	XXX
V4	2202	14	438	cohesive	XXX	XXX
H3 (2)	2202	14	924	partial adhesive	6 to 7	<31 (0.4Q)
H4 (2)	2202	14	527	cohesive	XXX	XXX

Table 16. Adhesion strength and surface characterization after CDT: CT #3 in 0.5M NaCl

Dolly Number (ID)	Epoxy	Dolly Size (mm)	PSI	Failure Type	Chemistry	
					pH	Cl- (ppm)
H1	8595	20	356	cohesive	XXX	XXX
H2	8595	20	628	cohesive	XXX	XXX
H3	8595	20	756	cohesive	XXX	XXX
H4	8595	20	XXX	XXX	XXX	XXX
V1	8595	20	376	partial adhesive	5.5	47.5 (1.7Q)
V2	8595	20	722	partial adhesive	8	<31 (0.1Q)
V3	8595	20	XXX	XXX	XXX	XXX
V4	8595	20	324	cohesive	XXX	XXX

Table 17. Adhesion strength and surface characterization after CDT: RCT #1 in 0.5M NaCl

Dolly Number (ID)	Epoxy	Dolly Size	Strength	Failure Type	Chemistry	
	Type	mm	psi		pH	Cl- (ppm)
H1	8595	20	191	cohesive	XXX	XXX
H2	8595	20	140	cohesive	XXX	XXX
V1	8595	20	176	cohesive	XXX	XXX
V2	8595	20	232	cohesive	XXX	XXX

Table 18. Adhesion strength and surface characterization after CDT: RCT #2 in 0.5M NaCl

Dolly Number (ID)	Epoxy	Dolly Size (mm)	PSI	Failure Type	Chemistry	
					pH	Cl- (ppm)
H1	8595	20	267	cohesive	XXX	XXX
H2	8595	20	332	cohesive	XXX	XXX
V1	8595	20	272	cohesive	XXX	XXX
V2	8595	20	276	cohesive	XXX	XXX

Table 19. Adhesion strength and surface characterization after CDT: FBE in soil.

Dolly Number (ID)	Epoxy	Dolly Size (mm)	PSI	Failure Type
C1 V1	8595	20	XXX	XXXXX
C1 V2	8595	20	XXX	XXXXX
C1 V3	2022	20	1586	partial adhesion
C1 V4	2022	20	XXX	XXXXX
C1 H1	2022	20	1552	epoxy
C1 H2	2022	20	1412	partial adhesion
C1 H3	8595	20	XXX	XXXXX
C1 H4	8595	20	708	epoxy
C2 V1	8595	20	XXX	XXXXX
C2 V2	8595	20	XXX	partial adhesion
C2 V3	2022	20	888	adhesion
C2 V4	2022	20	XXX	XXXXX
C2 H1	2022	20	XXX	XXXXX
C2 H2	2022	20	948	adhesion
C2 H3	8595	20	XXX	partial adhesion
C2 H4	8595	20	XXX	XXXXX

Table 20. Adhesion strength and surface characterization after CDT: CT in soil.

Dolly Number (ID)	Epoxy	Dolly Size (mm)	PSI	Failure Type
C1 V1	2022	20	XXX	XXXXX
C1 V2	2022	20	287	cohesive
C1 V3	8595	20	413	cohesive
C1 V4	8595	20	236	cohesive
C1 H1	8595	20	233	cohesive
C1 H2	8595	20	304	cohesive
C1 H3	2022	20	XXX	XXXXX
C1 H4	2022	20	XXX	XXXXX
C2 V1	8595	20	XXX	XXXXX
C2 V2	8595	20	382	cohesive
C2 V3	2022	20	324	cohesive
C2 V4	2022	20	468	cohesive
C2 H1	8595	20	386	cohesive
C2 H2	8595	20	201	cohesive
C2 H3	2022	20	378	cohesive
C2 H4	2022	20	XXX	XXXXX

Table 21. Ion Selective Chromatography results: FBE in 0.5 M NaCl. ND = Non-detectable.

Sample ID	Analyte Composition (ppm)						
	Fluoride	Chloride	Nitrite	Bromide	Nitrate	Phosphate	Sulfate
FBE 2 (#4)	0.51	3.25	ND	ND	ND	6.11	0.63
FBE 2 (#7)	2.14	ND	ND	ND	ND	0.82	ND
FBE 2 (#8)	0.43	5.21	ND	ND	0.35	ND	3.00
FBE 1	ND	2.66	ND	ND	7.57	2.07	ND
FBE V2	ND	10.60	ND	ND	ND	2.02	0.70

Table 22. Ion Selective Chromatography results: CT in 0.5 M NaCl. ND = Non-detectable

Sample ID	Analyte Composition (ppm)						
	Fluoride	Chloride	Nitrite	Bromide	Nitrate	Phosphate	Sulfate
CT3 H1	0.43	5.37	ND	ND	ND	30.70	0.24
CT3 H2	0.31	2.26	ND	ND	ND	ND	0.4
CT3 V1	ND	3.71	ND	ND	ND	0.91	0.17
CT3 V2	ND	4.42	ND	ND	ND	0.92	0.91
H3 2	0.51	14.2	ND	ND	ND	ND	ND
CT5 V1	0.6	1.03	ND	ND	ND	3.05	ND
CT5 V2	2.35	93.1	ND	ND	ND	6.12	0.88

Results obtained for aged FBE in both 0.5 M NaCl and soil environments were in line with the results obtained for new FBE coatings. Adhesion strength before testing always surpassed the strength of the adhesives used to attach the dollies. No failure of the FBE coating occurred before the CDT. After testing, however, failures were observed at locations near the defect from where hydrogen evolution was readily visible, Figure 31. Adhesion strength on failed spots varied from 362 to about 1600 psi. The surface pH was always near neutral and the chloride content below 31 ppm. IEC analysis (Table 21) confirmed the surface chemistry measured using the Bresle patches.

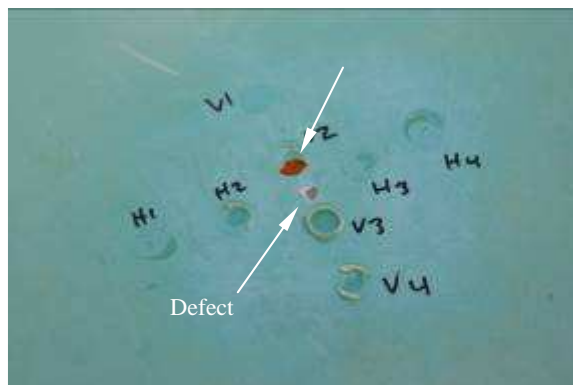


Figure 31. Pull-off adhesion measurements showing a failed spot near the defect.

Results obtained for CTE samples in NaCl showed that after CDT, the failure mode near the holiday changed from purely cohesive to adhesive, indicating the degradation of the bond between the steel and the coating (Figure 32). Adhesion strength varied from about 300 to 700 psi. In RCTE samples, areas where partial coating removal was observed occurred near the defect.

However, the overall response of the RCT was better than that of CTE coatings as the main failure mode was cohesive. The pH on the failed areas was nearly neutral and the chloride content below 31 ppm. IEC analysis confirmed the chloride contents measured with the Bresle patches. Only two locations showed elevated chloride contents of 14 and 93 ppm compared to all other locations that were less than 5.4 ppm.



Figure 32. Pull-off adhesion measurements showing a failed spot near the defect.

In contrast to 0.5 M NaCl, no adhesive failure was observed in CTE samples exposed to soil. This was probably a consequence of the shorter exposure time and lower conductivity (and thus lower current density for the same level of polarization). All the failures were cohesive with pull-off values between 140 and 400 psi.

4.1.3 CDT on flat coupons

Similar to the tests on new FBE pipe sections, an evaluation of the effects of prior surface condition on the rate of coating disbondment when using coatings commonly utilized for patch jobs in the field was performed. As previously described, samples were cathodically protected using an Mg anode and a defect was introduced according to ASTM G 95. Under these conditions accelerated failure of the coating was expected. Figure 33 shows the actual setup.

Pipe steel coupons were prepared with two surface finishes and three different types of surface contamination. The choice of surface finish and contamination were based on the previous work conducted at DNV Columbus (at the time CC Technologies) by Ruschau, et al. [9]. Table 23 summarizes the selected surface conditions.

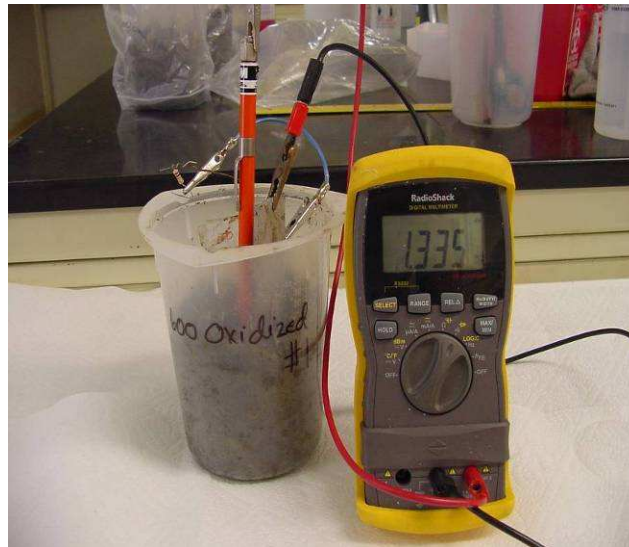


Figure 33. Test assembly for the modified ASTM G 8 procedure B using an Mg anode.

Table 23. Matrix summarizing the experimental approach.

Coating Type	Surface Finishing	# Replicates	Sample Dimensions
Water repellant Epoxy	White Sandblasted (SB)	2	3" x 3"
	SB Cl Contaminated (C)	2	3" x 3"
	SB Mud (MG)	2	3" x 3"
	600 grit (6G)	2	3" x 3"
Water repellant Epoxy	600 grit Cl contaminated (6GC)	2	3" x 3"
	6G Mud (6GM)	2	3" x 3"

Coupons were made of 5LX65 pipe steel. To introduce chloride or mud contamination, samples were first pre-heated on a hot plate. Hot samples were removed from the plate and immediately sprayed with a 0.5 M NaCl aqueous electrolyte or dipped in a beaker containing a liquid mud slurry. The chloride and pH concentration of the surface was characterized by testing spare samples following the same procedures. Each measurement was repeated at least in triplicate. The visual appearance of pre-treated samples is shown in Figure 34 and Figure 35. Coating application was made in the laboratory using commercially available water repellant epoxy products. Coating was applied using a roller and allowed to cure for 48 h before testing.

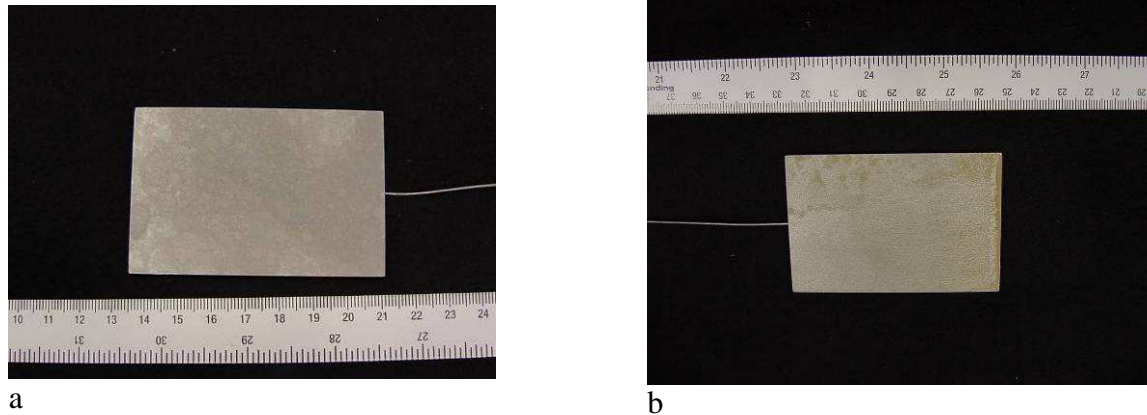


Figure 34. Visual appearance of sand blasted coupons after: a) chloride and b) mud contamination

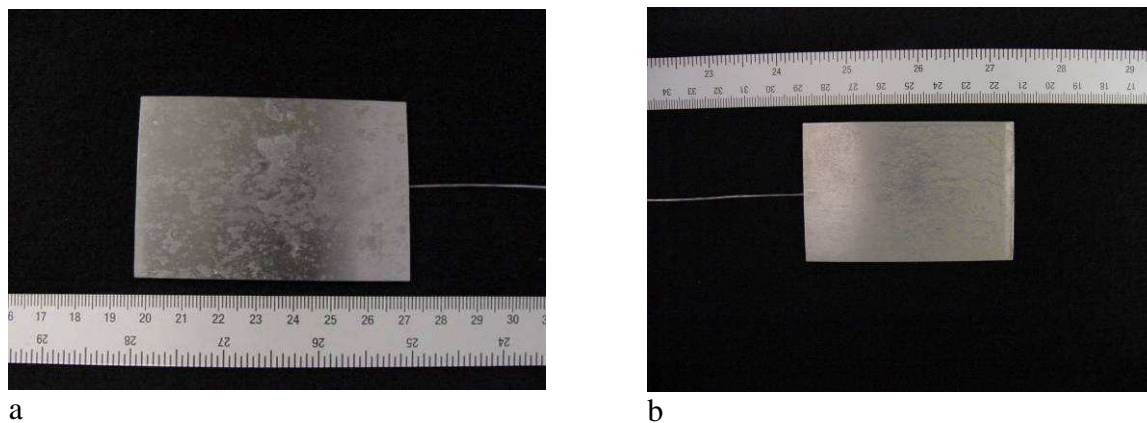


Figure 35. Visual appearance of 600 grit coupons after: a) chloride and b) mud contamination

After pre-treatment, a set of samples was analyzed following the standardized procedure described previously. Table 24 summarizes the average chloride and pH values for the different pre-treatments. Surfaces were also replicated using the Struers Repliset kit for posterior analysis. Figure 36 shows the differences in surface topography as evidenced by optical microscopy.

Table 24. Matrix summarizing the proposed experimental approach.

Surface Finishing/ Pre-treatment	pH	Cl [ppm]	Testex Profile [mils]
Sand Blast/ As Received	5	< 31	1.5
Sand Blast/ Chloride	4-5	207	
Sand Blast/ Mud	5	< 31	
600 Grit/ As Received	5	< 31	0.95
600 Grit/ Chloride	4-5	108	
600 Grit/ Mud	5	< 31	

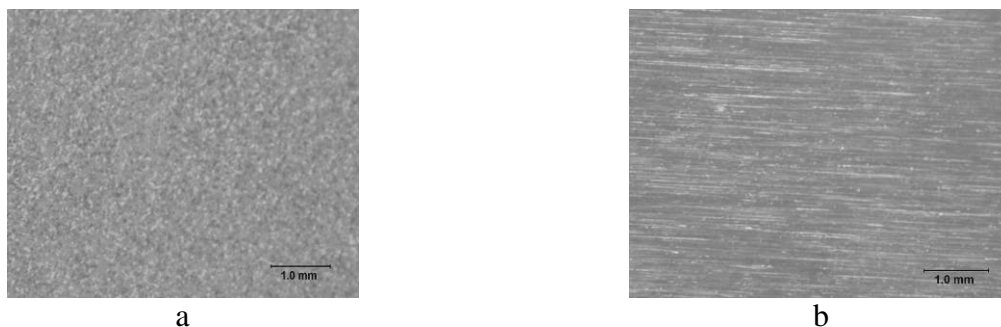


Figure 36. Optical stereo-micrographs of the replicated surface of: a) sand blast and b) 600 grit coupons.

The soil pH and the *on* and instant-*off* potentials were monitored on a weekly basis. Electrochemical impedance spectroscopy (EIS) was conducted periodically to evaluate the degree of water uptake in the coatings and to detect overall coating deterioration. No complex EIS modeling was conducted. Parameters that have been connected with coating degradation, such as low frequency impedance and phase angle, were used to provide a picture of coating performance.

The soil resistivity was adjusted to 700-1000 Ω -cm and monitored periodically. Soil resistivity was adjusted if necessary. Figure 37 shows the average time evolution of the soil resistivity. Results of soil pH measurements are shown in Figure 38. Soil pH remained approximately constant at about 7.

As shown in Figure 39, the steady state *on* potential for all the samples, with the exception of the oxide pre-treated 600-grit sample, was approximately -1.3 to -1.35 V vs Cu/CuSO₄. The oxide covered 600 grit sample showed a large dispersion in the *on* potential. However, these oscillations were more negative than the -950 mV criterion. The steady state instant-*off* potential had a larger variability but it averaged about -0.7 V vs Cu/CuSO₄.

Results of the low frequency impedance (LFI) magnitude at 10 mHz are illustrated in Figure 40. Initially, all samples showed a large dispersion in LFI values with no clear trend when comparing the effects of surface finish and pretreatment. Initial LFI values were relatively high, in general ranging from 0.6 to 1 $M\Omega - cm^2$. In both the white sand blast and 600 grit finish cases, the oxide covered surface reached LFI values above 1 $M\Omega - cm^2$. After 45 days, however, the LFI of all samples for both surface finishes dropped considerably and remained low for the duration of the test. This seems to indicate that after 45 days, the coatings have disbonded.

Samples were removed after 90 days and characterized following the procedures described previously. Results of pull-off adhesion tests as well as pH and chloride measurements are summarized in Figures 41 to 44.

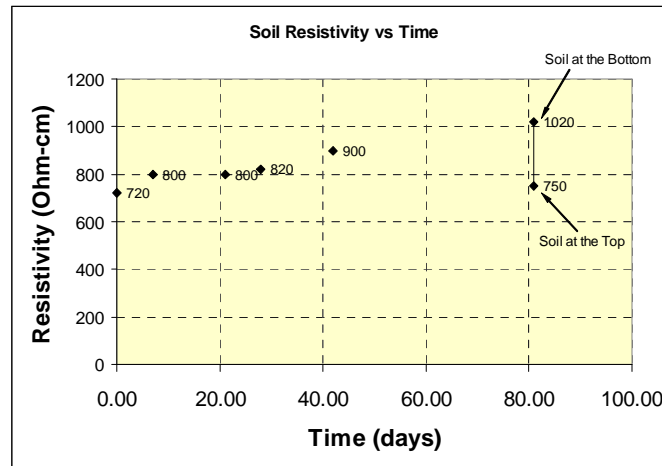


Figure 37. Soil resistivity as a function of exposure time.

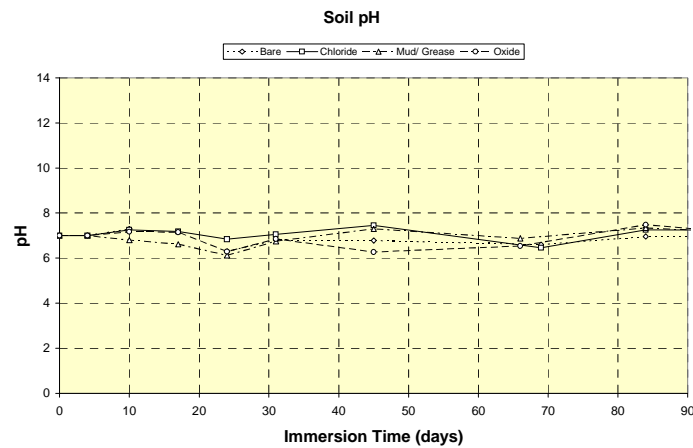


Figure 38. Soil pH as a function of exposure time.

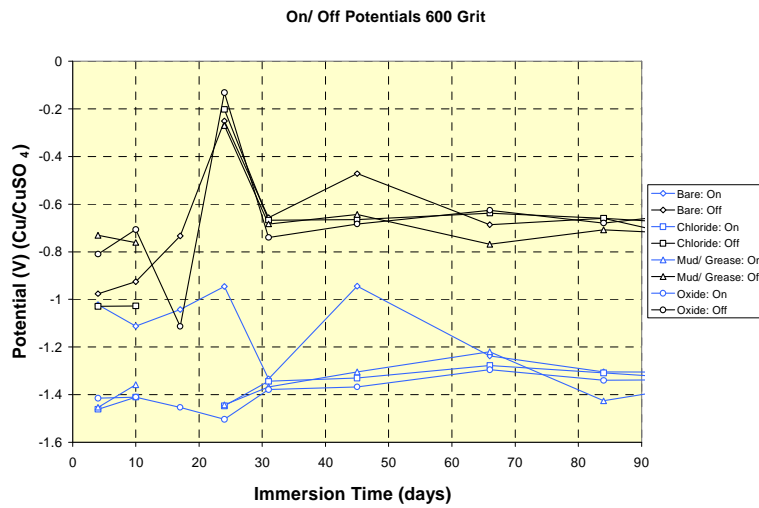
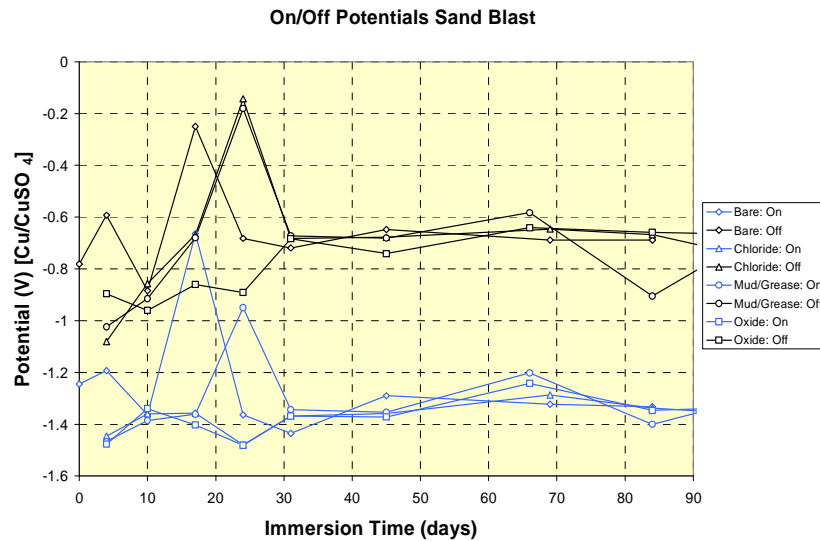


Figure 39. On and instant off potentials vs time: a) white sand blast and b) 600 grit.

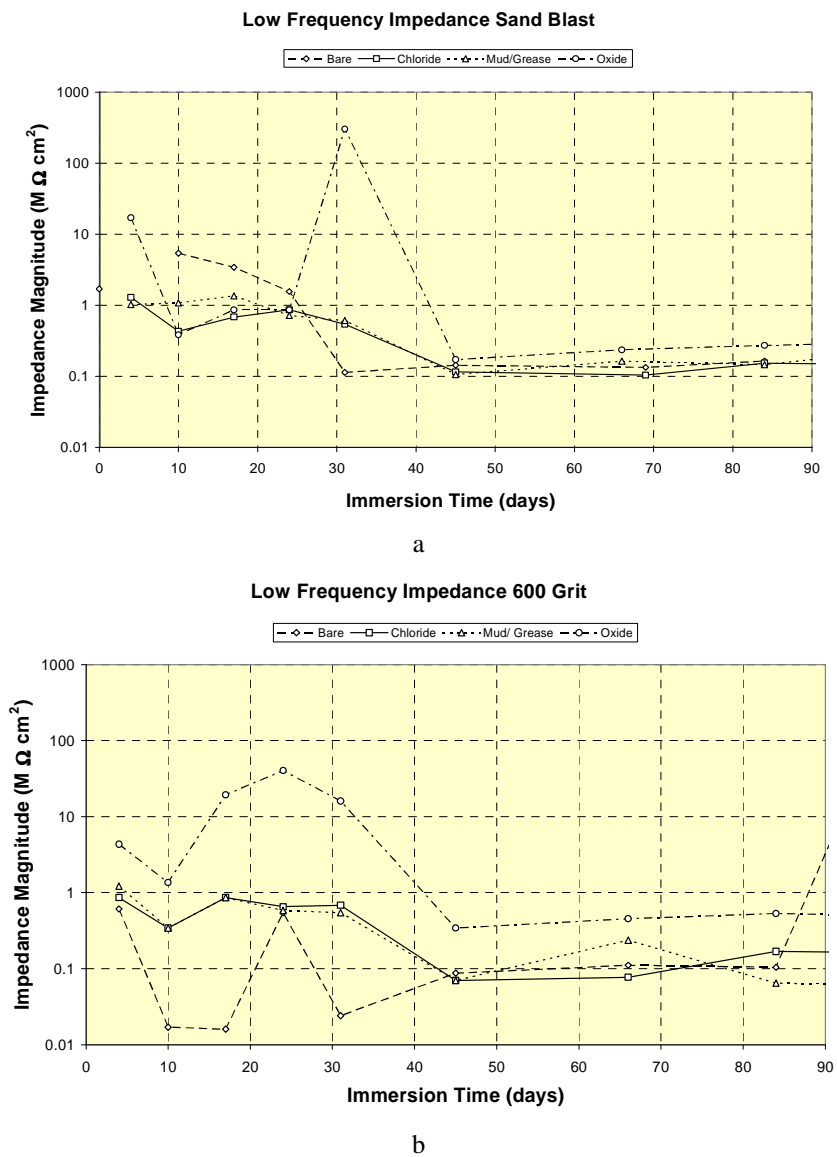


Figure 40. LFI magnitude vs time: a) white sand blast and b) 600 grit.

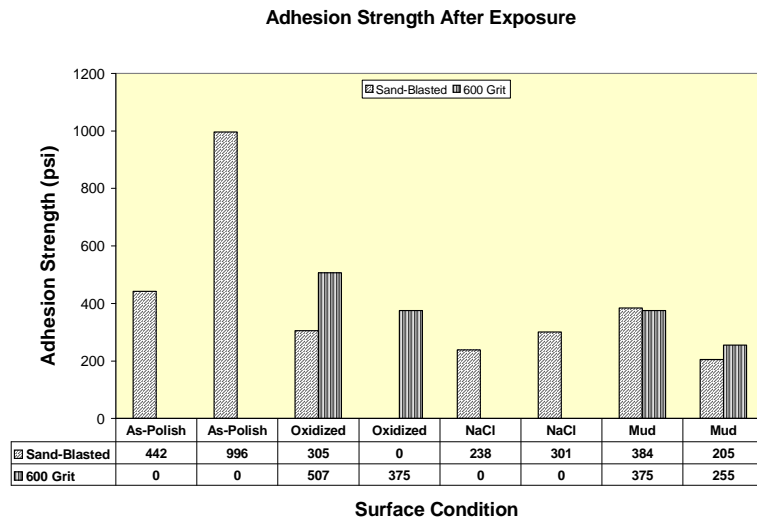


Figure 41. Adhesion strength as a function of surface pre-treatment.

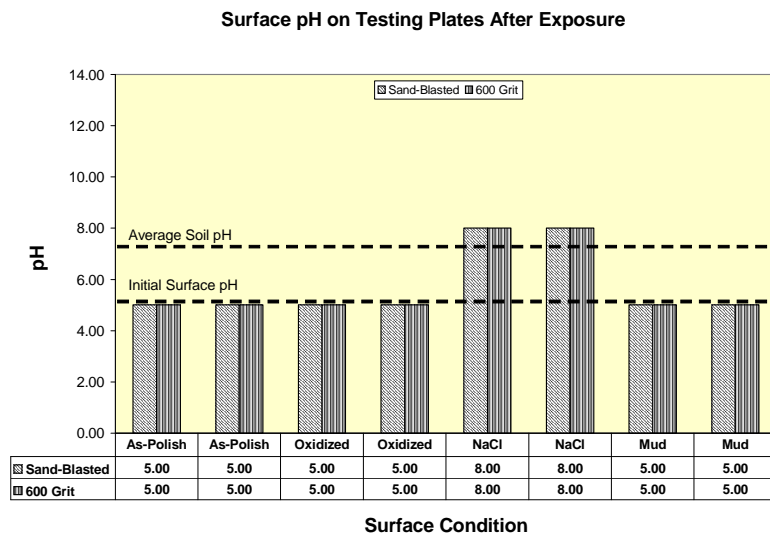


Figure 42. Surface pH on testing plates as a function of surface pre-treatment.

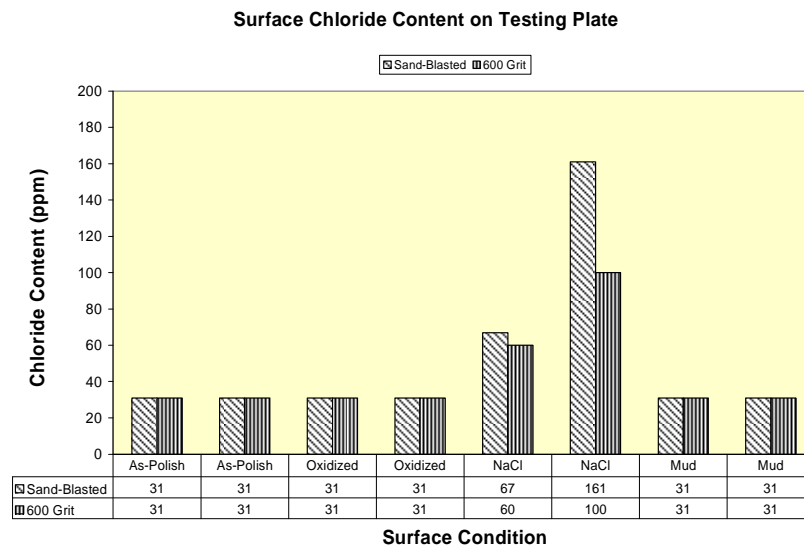


Figure 43. Chloride content on testing plates as a function of surface pre-treatment.

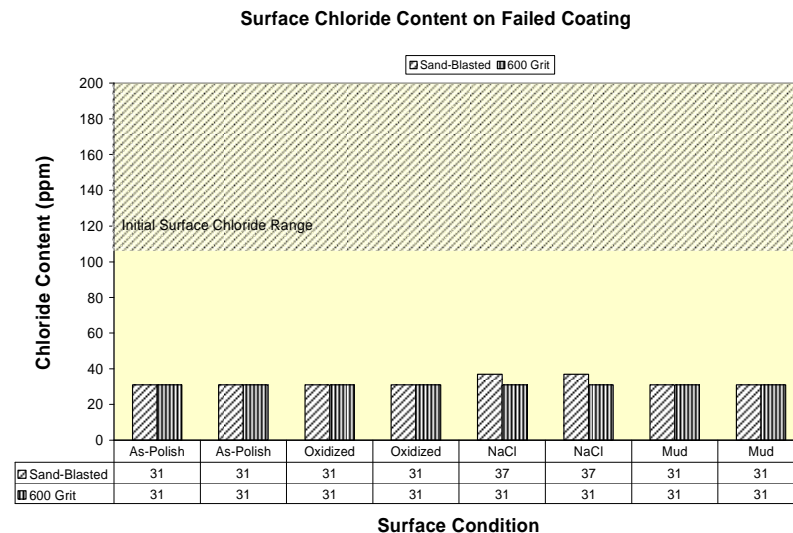


Figure 44. Chloride content on the back of the failed coatings as a function of surface pre-treatment.

The first observation to make is that the adhesion strength of this type of epoxy coating was significantly lower than what was seen for FBE samples. The maximum adhesion strength after testing reached only 1000 psi on a sand blasted surface with no pre-treatment, which would be considered to be the most ideal case. Furthermore, several samples failed during setup, indicating that the coatings were completely disbonded even prior to the initiation of testing. With this caveat in mind, the as-received white sand blast sample showed the highest adhesion strength. Likewise, chloride surface contamination consistently gave the lowest values.

The surface chemistry analysis was in line with the data presented so far. The pH was approximately neutral, except for the intentional chloride contamination surface pre-treatment where the pH was 8. However, no changes in surface chloride were observed after exposure.

5 ON-SITE ANALYSIS

In order to improve confidence and validate the procedure developed to assess laboratory applied coatings, on-site evaluations of in-service pipeline coating disbondments were conducted. The first excavation took place in Louisiana during the first week of January 2007. According to the data surveyed by DNV Columbus, the site presented signs of possible coating failure. Even when signs of coating failure were encountered as seen in Figure 45, the location and the wrinkled conditions of the coating made adhesion measurements impossible. Even though no tests were conducted, this experience showed the typical difficulties that on-site analysis could face.



Figure 45. General and specific view of the excavation conducted by DNV COLUMBUS in Louisiana during January 2007

The second excavation took place in Maryland during August 2007. This pipeline transported liquid petroleum and had an estimated age of over 50 years. The pipe had a coal tar enamel coating and aboveground potential surveys suggested that coating disbondments were present. A picture of the site prior to analysis is shown in Figure 46. The pipe was scheduled to be recoated. The analysis was coordinated to take place before the removal of the entire coating.



Figure 46. Pipe section before analysis.

The pipe section was analyzed following the test protocol presented previously. The first step was the removal of the tape wrap that covered the coal tar coating (Figure 47). After removing the tape, the coal tar surface was cleaned and dollies applied using either Araldite 8595 or 2202 epoxy adhesives as shown in Figure 48. Dollies were placed in the 12, 3(9), and 6 O'clock positions.



Figure 47. Tape covering the coal tar surface was removed before testing.



Figure 48. 50 mm dolly applied at the 12 o'clock position.

The pipe had visible signs of coating deterioration. In some places water was found inside disbonded areas (Figure 49), similar to what was observed in the laboratory scale testing on reinforced coal tar pipe samples. Chemical analysis was conducted on site and samples were also brought to the laboratory to determine the composition of the water by chromatography. In the areas where coating damaged was evident, all the loose coating was first removed with a utility knife (Figure 50). The analysis was conducted in areas adjacent to the damaged region.

In total, more than 100 dollies (diameters: 50, 20 and 14 mm) were applied on the surface of the pipe. Some problems arose during the last 2 days of testing due to the build up of water inside the ditch. Water was removed later with a pump but by the time some dollies located at the 6 o'clock position had been submerged and were washed away (Figure 51). Table 25 to Table 28 summarize the pull off adhesion results for one of the sections. As shown in Table 25 most of the failures were cohesive, even in the proximities of coating defects. Since the coal tar enamel coatings systematically showed cohesive failure, the coating was then removed by hammering and scraping of the coating. Table 29 summarized the results of the on site chemistry analysis. Samples of the ground and running water were also analyzed.



Figure 49. Signs of coating damaged were found at different locations.



Figure 50. Removal of damaged coal tar coating prior to analysis on the areas adjacent to the defects.



Figure 51. Water flooded the ditch, removing some of the dollies located at the 6 o'clock position.

Table 25. Pull off adhesion results for pipe section 1.

Date/Time Dolly Applied	Date/Time Dolly Pulled	Dolly Number (ID)	Epoxy	Dolly Size (mm)	Clock Position (o'clock)	PSI	Failure Type
A.M. Rain; P.M. Sunny Temp:92.3 RH:98.5%	P.M. Sunny Temp:94.8 RH:50.7%						
8/16/2007 Afternoon	8/17/2007 Afternoon	S1#1	8595	50	12	188	cohesive
8/16/2007 Afternoon	8/17/2007 Afternoon	S1#2	8595	20	12	284	cohesive
8/16/2007 Afternoon	8/17/2007 Afternoon	S1#3	8595	50	12	276	cohesive
8/16/2007 Afternoon	8/17/2007 Afternoon	S1#4	8595	20	12	331	cohesive
8/16/2007 Afternoon	8/17/2007 Afternoon	S1#5	8595	20	12	109	cohesive
8/16/2007 Afternoon	8/17/2007 Afternoon	S1#1	2022	50	12	>1200	cohesive
8/16/2007 Afternoon	8/17/2007 Afternoon	S1#2	2022	20	12	288	cohesive
8/16/2007 Afternoon	8/17/2007 Afternoon	S1#3	2022	20	3	185	cohesive
8/16/2007 Afternoon	8/17/2007 Afternoon	S1#4	2022	50	12	214	cohesive
8/16/2007 Afternoon	8/17/2007 Afternoon	S1#5	2022	20	12	444	cohesive
8/16/2007 Afternoon	8/17/2007 Afternoon	S1#6	2022	50	12	XXX	XXXXXXX
8/16/2007 Afternoon	8/17/2007 Afternoon	S1#7	2022	20	12	458	cohesive
8/16/2007 Afternoon	8/17/2007 Afternoon	S1#8	2022	50	12	180	cohesive

Table 26. Pull off adhesion results for pipe section 2.

Date/Time Dolly Applied	Date/Time Dolly Pulled	Dolly Number (ID)	Epoxy	Dolly Size (mm)	Clock Position (o'clock)	PSI	Failure Type
A.M. Rain; P.M. Sunny Temp:92.3 RH:98.5%	P.M. Sunny Temp:94.8 RH:50.7%						
8/16/2007 Afternoon	8/17/2007 Afternoon	S2#1	8595	50	12	313	cohesive
8/16/2007 Afternoon	8/17/2007 Afternoon	S2#2	8595	20	12	332	cohesive
8/16/2007 Afternoon	8/17/2007 Afternoon	S2#3	8595	50	12	336	cohesive
8/16/2007 Afternoon	8/17/2007 Afternoon	S2#4	8595	20	12	336	cohesive
8/16/2007 Afternoon	8/17/2007 Afternoon	S2#5	8595	20	12	331	cohesive
8/16/2007 Afternoon	8/17/2007 Afternoon	S2#6	8595	50	12	312	cohesive
8/16/2007 Afternoon	8/17/2007 Afternoon	S2#7	8595	20	9	76	cohesive
8/16/2007 Afternoon	8/17/2007 Afternoon	S2#8	8595	20	3	XXX	XXXXXXX
8/16/2007 Afternoon	8/17/2007 Afternoon	S2#9	8595	20	3	XXX	XXXXXXX
8/16/2007 Afternoon	8/17/2007 Afternoon	S2#10	8595	20	3	XXX	XXXXXXX
8/16/2007 Afternoon	8/17/2007 Afternoon	S2#1	2022	50	12	231	cohesive
8/16/2007 Afternoon	8/17/2007 Afternoon	S2#2	2022	20	12	405	cohesive
8/16/2007 Afternoon	8/17/2007 Afternoon	S2#3	2022	50	12	119	cohesive
8/16/2007 Afternoon	8/17/2007 Afternoon	S2#4	2022	20	12	435	cohesive
8/16/2007 Afternoon	8/17/2007 Afternoon	S2#5	2022	50	12	153	cohesive
8/16/2007 Afternoon	8/17/2007 Afternoon	S2#6	2022	20	9	318	cohesive

Table 27. Pull off adhesion results for pipe section 3.

Date/Time Dolly Applied	Date/Time Dolly Pulled	Dolly Number (ID)	Epoxy	Dolly Size (mm)	Clock Position (o'clock)	PSI	Failure Type
A.M. Rain; P.M. Sunny Temp:92.3 RH:98.5%	P.M. Sunny Temp:94.8 RH:50.7%						
8/16/2007 Afternoon	8/17/2007 Afternoon	S3#1	8595	20	12	117	cohesive
8/16/2007 Afternoon	8/17/2007 Afternoon	S3#2	8595	50	12	276	cohesive
8/16/2007 Afternoon	8/17/2007 Afternoon	S3#3	8595	50	9	205	cohesive
8/16/2007 Afternoon	8/17/2007 Afternoon	S3#4	8595	50	12	225	cohesive
8/16/2007 Afternoon	8/17/2007 Afternoon	S3#5	8595	20	12	123	cohesive
8/16/2007 Afternoon	8/17/2007 Afternoon	S3#6	8595	20	3	239	cohesive
8/16/2007 Afternoon	8/17/2007 Afternoon	S3#7	8595	20	3	343	cohesive
8/16/2007 Afternoon	8/17/2007 Afternoon	S3#8	8595	50	3	280	cohesive
8/16/2007 Afternoon	8/17/2007 Afternoon	S3#1	2022	20	12	418	cohesive
8/16/2007 Afternoon	8/17/2007 Afternoon	S3#2	2022	50	12	245	cohesive
8/16/2007 Afternoon	8/17/2007 Afternoon	S3#3	2022	50	9	32	cohesive
8/16/2007 Afternoon	8/17/2007 Afternoon	S3#4	2022	50	12	231	cohesive
8/16/2007 Afternoon	8/17/2007 Afternoon	S3#5	2022	20	12	270	cohesive
8/16/2007 Afternoon	8/17/2007 Afternoon	S3#6	2022	20	6	239	cohesive
8/16/2007 Afternoon	8/17/2007 Afternoon	S3#7	2022	20	3	243	cohesive
8/16/2007 Afternoon	8/17/2007 Afternoon	S3#8	2022	50	3	155	cohesive

Table 28. Pull off adhesion results for pipe section 4.

Date/Time Dolly Applied	Date/Time Dolly Pulled	Dolly Number (ID)	Epoxy	Dolly Size (mm)	Clock Position (o'clock)	PSI	Failure Type
A.M. Rain; P.M. Sunny Temp:92.3 RH:98.5%	P.M. Sunny Temp:94.8 RH:50.7%						
8/16/2007 Afternoon	8/17/2007 Afternoon	S4#1	8595	20	12	350	cohesive
8/16/2007 Afternoon	8/17/2007 Afternoon	S4#2	8595	50	12	303	cohesive
8/16/2007 Afternoon	8/17/2007 Afternoon	S4#3	8595	50	12	287	cohesive
8/16/2007 Afternoon	8/17/2007 Afternoon	S4#4	8595	20	12	412	cohesive
8/16/2007 Afternoon	8/17/2007 Afternoon	S4#5	8595	20	9	180	cohesive
8/16/2007 Afternoon	8/17/2007 Afternoon	S4#6	8595	20	9	130	cohesive
8/16/2007 Afternoon	8/17/2007 Afternoon	S4#7	8595	20	9	165	cohesive
8/16/2007 Afternoon	8/17/2007 Afternoon	S4#8	8595	20	9	XXX	XXXXXXX
8/16/2007 Afternoon	8/17/2007 Afternoon	S4#9	8595	50	12	200	cohesive
8/16/2007 Afternoon	8/17/2007 Afternoon	S4#10	8595	20	12	385	cohesive
8/16/2007 Afternoon	8/17/2007 Afternoon	S4#11	8595	20	3	300	cohesive
8/16/2007 Afternoon	8/17/2007 Afternoon	S4#12	8595	50	3	277	cohesive
8/16/2007 Afternoon	8/17/2007 Afternoon	S4#1	2022	20	12	452	cohesive
8/16/2007 Afternoon	8/17/2007 Afternoon	S4#2	2022	50	12	294	cohesive
8/16/2007 Afternoon	8/17/2007 Afternoon	S4#3	2022	50	12	232	cohesive
8/16/2007 Afternoon	8/17/2007 Afternoon	S4#4	2022	20	12	515	cohesive
8/16/2007 Afternoon	8/17/2007 Afternoon	S4#5	2022	50	12	194	cohesive
8/16/2007 Afternoon	8/17/2007 Afternoon	S4#6	2022	20	12	332	cohesive
8/16/2007 Afternoon	8/17/2007 Afternoon	S4#7	2022	20	3	425	cohesive
8/16/2007 Afternoon	8/17/2007 Afternoon	S4#8	2022	50	3	XXX	XXXXXXX

Table 29. On site chemistry analysis.

Sample Number (ID)	Sample Description	Chemistry	
		pH	Cl (ppm)
S1#1	Running Water	6.5	<31 (0.5Q)
S1#2	Ground Water 1	5.5	<31 (0.6Q)
S1#3	Ground Water 2	6	<31 (0.5Q)
S2#1	Running Water	6	<31 (0.7Q)
S2#2	Ground Water 1	6	<31 (0.5Q)
S2#3	Ground Water 2	5.5	<31 (0.6Q)
S3#1	Running Water	6	<31 (0.5Q)
S3#2	Ground Water 1	6	<31 (0.6Q)
S3#3	Ground Water 2	5.5	<31 (0.6Q)
S4#1	Ground Water 1	6.5	<31 (0.6Q)
S4#2	Ground Water 2	6	<31 (0.6Q)
S4#3	9 Inch Blister 1	4.5	<31 (0Q)
S4#4	9 Inch Blister 2	5	<31 (0Q)
S4#5	Exposed Area	5	<31 (0.1Q)
S4#6	Blister Surface Cut-Out	5	<31 (0Q)

6 DISCUSSION

Although several techniques have been developed to determine the extent of disbondment, the initiation stages remain unclear as yet. The original scope of this investigation was the analysis of aged pipe sections suspected of having coating disbondments. During the survey of available samples it was concluded that all the pipes at the DNV Columbus inventory primarily had intact FBE and CT coatings. This observation was made after analyzing, in total, more than 200 adhesion tests on varied pipe sections. This was probably due to the fact that during a typical

failure investigation, all the coating near the affected area is removed. Moreover, many times this is done in the field before the pipe sections actually reach the laboratory.

Adhesion strength of intact FBE coatings was systematically above the maximum strength of the adhesive used to attach the dollies to the pipe surface. Likewise, CTE and RCTE samples always showed cohesive failures, indicating that adhesion between the steel substrate and the coating was not degraded. As explained in the introduction, cohesive failures are preferred over adhesive failures as the failed coating can still provide some degree of protection. A completely adhesive failure indicates that the bond between the coating and the pipe steel were broken. Analysis of the conditions leading to good performance revealed that when the pipe sections had a white-sand-blasted surface good adhesion was consistently achieved. In addition, surface pH was always about neutral and the chloride concentration below 31 ppm.

To explain the onset of coating disbondment, there seems to be two prevailing theories: i) degradation of the bond between the steel substrate and the coating due to the development of an alkaline environment and ii) blistering due to production of $H_2(g)$. Both of these have documented experimental evidence to support them. These two possibilities are based on the environment evolving from the electrochemical reactions occurring at sufficiently high cathodic potentials. Different models based on observational evidence have been proposed to predict the ionic migration of species in and out of the disbondment, migration through the coating, and other processes. However, all these models tend to assume that a crevice (disbondment) is already present that can then facilitate the separation of anodic and cathodic reactions.

Experiments conducted in the lab using both new and aged pipe sections showed that the pH away from the defect remained near neutral. In addition, there were no measurable changes in chloride content as determined by titration and IEC. Although a poorly applied coating should not be ruled out, the extent of the attack observed on the new pipe sections in the as-received condition suggested that the disbondment extended beyond the exposed area. Coating samples from failed areas of FBE and coal tar sections, including those extracted from the field, were sent for Fourier Transformed Infrared (FTIR) Spectroscopy. According to the laboratory report FBE and CTE coatings showed no signs of oxidation when compared against the spectra of unexposed epoxy and coal tar control samples. The report also suggested that deposits commonly found in the base of the failed FBE coatings were magnesium carbonate and iron oxide.

These observations combined with the neutral pH found away from the defect cannot be explained by alkaline attack or by blistering caused by $H_2(g)$. More research is necessary to determine what other factors could cause the initial loss of adhesion. That is, what are the steps and mechanisms involved in the very nascent stages of coating disbondment. No doubt that alkalization and hydrogen evolution are present and associated with disbondments but it seems possible that these phenomena might prevail in the later stages of disbondment initiation or perhaps only during disbondment propagation. However, it is clear that current and

modifications of current testing methodologies are not suitable to determine the onset of coating disbondment.

Finally, it is important to highlight the poor performance of the water resistance epoxy coatings used in this investigation. Adhesion strength after CDT even in the as-received coupons was less than 1000 psi, which is lower than the lowest values measured for FBE coatings even with surface contamination.

7 CONCLUSIONS

In this project laboratory-generated results were compared to coating failures observed on pipe segments that had been taken out of service as well as in-ditch evaluations. By examining variables such as coating chemistry, surface chemistry and contamination, surface roughness, and anchor pattern a standardized experimental procedure aimed to evaluate the main causes leading to coating disbondment was developed and validated. Using this approach, the following conclusions were made:

1. Areas affected by cathodic disbondment on fusion bonded epoxy and coal tar enamel coatings tended to also exhibit low adhesion strength.
2. Highly alkaline conditions, as has been proposed to aid in the disbondment process, were observed during cathodic disbondment tests but only in the region immediately adjacent to the defect. At even small distances away from the defect, the pH was nearly neutral.
3. During cathodic disbondment testing, the disbondment often times extended beyond the initial exposed area of the test.

8 REFERENCES

1. G.S. Sergi and G.K. Glass, *Corr. Sci.* 42 (200): p: 2043
2. N.P. Glazov, *Protec. Metals* 40 (2004): p: 552
3. N. Kamalanand *et al.*, *Anti-Corr Meth. Mat.* 45 (1998): p:243
4. J.S. McHattie, I.L. Perez, and J.A. Kher, *Cement and Concrete Comp.* 18 (1996): p: 93
5. L.D. Vincent, *Mat Perform.* May (2002): p: 28
6. J.J. Perdomo and I. Song, *Corr. Sci.* 42 (2000): p: 1389
7. F.M. Song *et al.*, *Mat. Perform.* September (2003): p: 24
8. D-T Chin and G.M. Sabde, *Corrosion* 55 (1999): p: 3

-
9. C. G. Munger, "Corrosion Prevention by Protective Coatings", 2nd Edition, L. D. Vincent Revision Author, NACE (1999): p. 200.
 10. G. Ruschau, PRCI Final Report, Contract PR-186-03133, Dublin, OH (2006).
 11. N. Sridhar, "Modeling the conditions under disbonded coating crevices- A review", Southwest Research Institute Communication (1999).
 12. F. M. Song, N. Sridhar, *Corr. Sci.* 50 (2008): p. 70-83.
 13. F. M. Song, N. Sridhar, *Corrosion* 64, 1 (2208): p. 40-49.
 14. F. M. Song, N. Sridhar, *Corrosion* 62, 8 (2006) : p. 676-686.
 15. D. -T Chin, G. M. Sabde, "Modeling Transport Processes in a Cathodically Protected Crevice Beneath Disbonded Coating Holidays", CORROSION/99, paper no. 8Z.5 (Houston, TX: NACE International, 1999).
 16. X. Campaignolle, S. Gastaud, S. Karcher, M. Meyer, "Corrosion of Pipelines Under CP in the Presence of Coating Disbonding", EUROCORR/2004, paper no. 074 (Nice, France: European Federation of Corrosion, 2004).

- oOo -

DNV Energy

DNV Energy is a leading professional service provider in safeguarding and improving business performance, assisting energy companies along the entire value chain from concept selection through exploration, production, transportation, refining and distribution. Our broad expertise covers Asset Risk & Operations Management, Enterprise Risk Management; IT Risk Management; Offshore Classification; Safety, Health and Environmental Risk Management; Technology Qualification; and Verification.

DNV Energy Regional Offices:

Asia and Middle East

Det Norske Veritas Sdn Bhd
24th Floor, Menara Weld
Jalan Raja Chulan
50200 Kuala Lumpur
Phone: +603 2050 2888

North America

Det Norske Veritas (USA), Inc.
1400 Ravello Dr.
Katy, TX 77449
United States of America
Phone: +281 396 1000

Europe and North Africa

Det Norske Veritas Ltd
Palace House
3 Cathedral Street
London SE1 9DE
United Kingdom
Phone: +44 20 7357 6080

Offshore Class and Inspection

Det Norske Veritas AS
Veritasveien 1
N-1322 Hovik
Norway
Phone: +47 67 57 99 00

Cleaner Energy & Utilities

Det Norske Veritas AS
Veritasveien 1
N-1322 Hovik
Norway
Phone: +47 67 57 99 00

South America and West Africa

Det Norske Veritas Ltda
Rua Sete de Setembro
111/12 Floor
20050006 Rio de Janeiro Brazil
Phone: +55 21 2517 7232

Nordic and Eurasia

Det Norske Veritas AS
Veritasveien 1
N-1322 Hovik
Norway
Phone: +47 67 57 99 00